Inverse Transport and Optical Tomography

John C Schotland
Mathematics Department
University of Michigan

schotland@umich.edu

Joint work with Manabu Machida, Vadim Markel and George Panasyuk

Experiments by Soren Konecky and Zhengmin Wang

A simple experiment

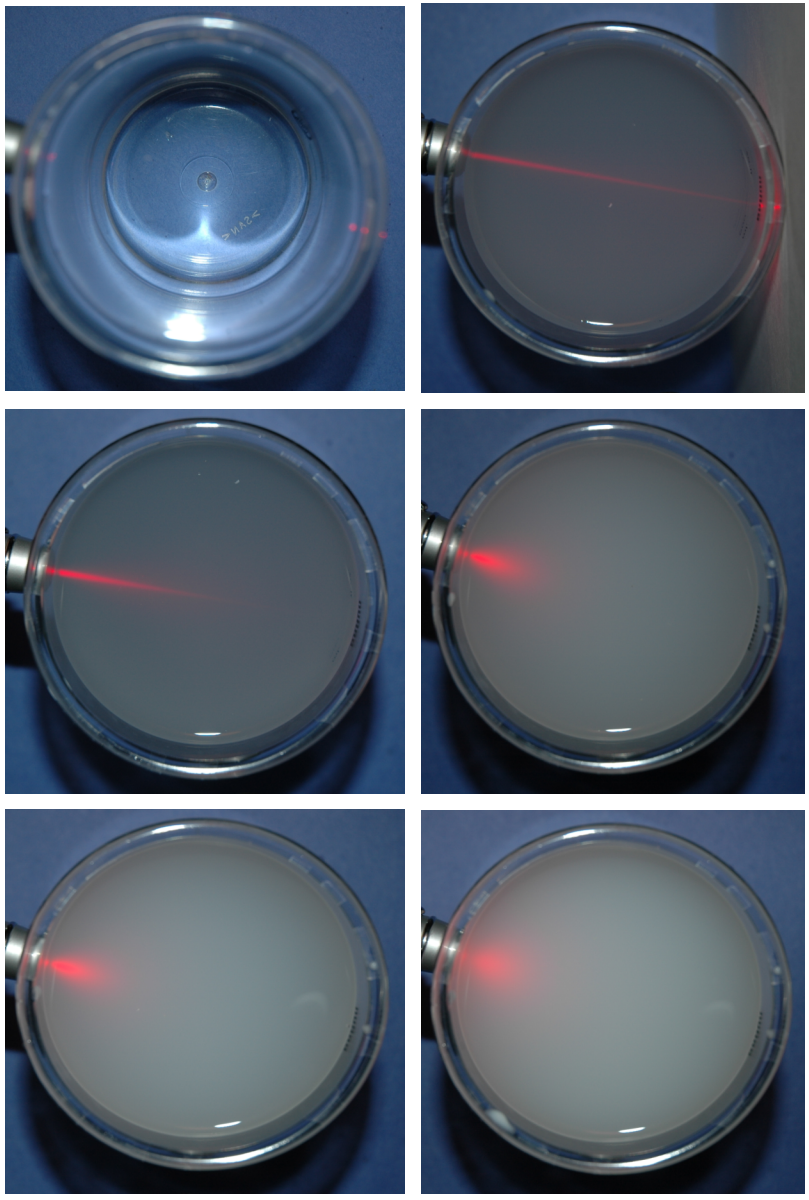

Geometrical optics

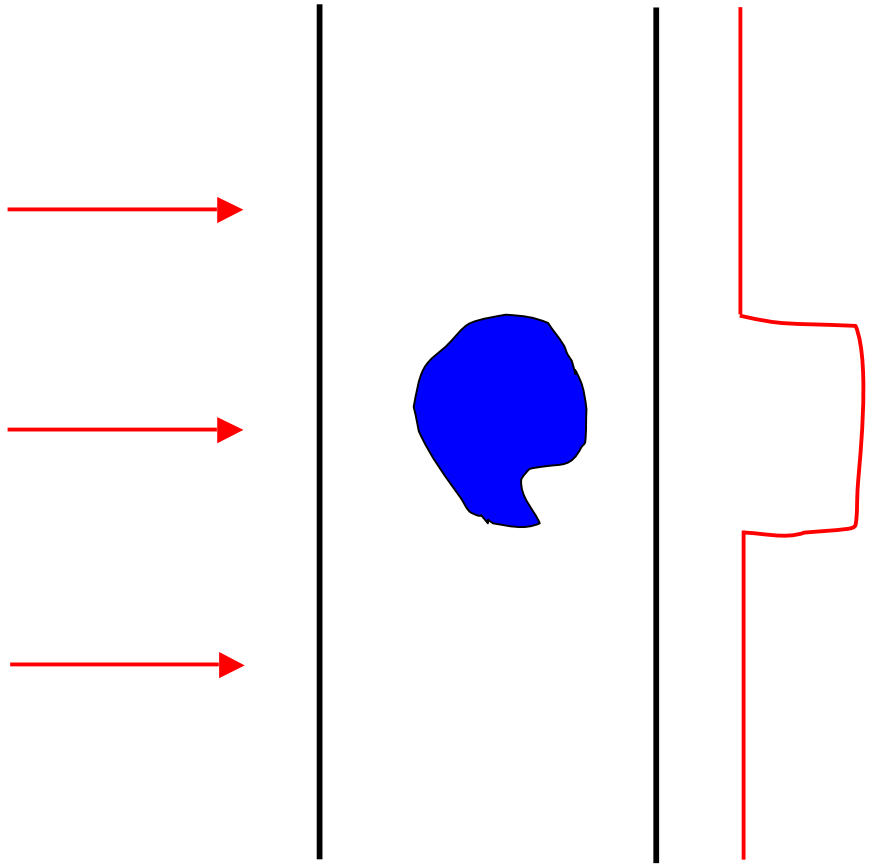

$L \ll \ell_s$

Weak scattering

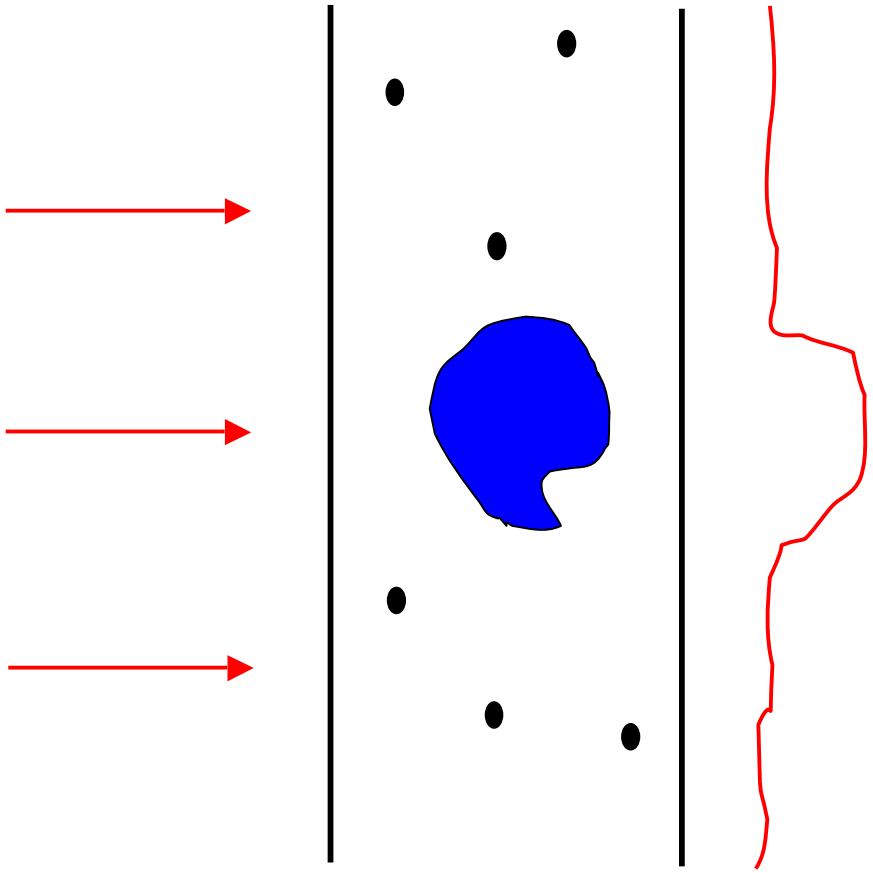

$L \sim \ell_s$

Strong scattering

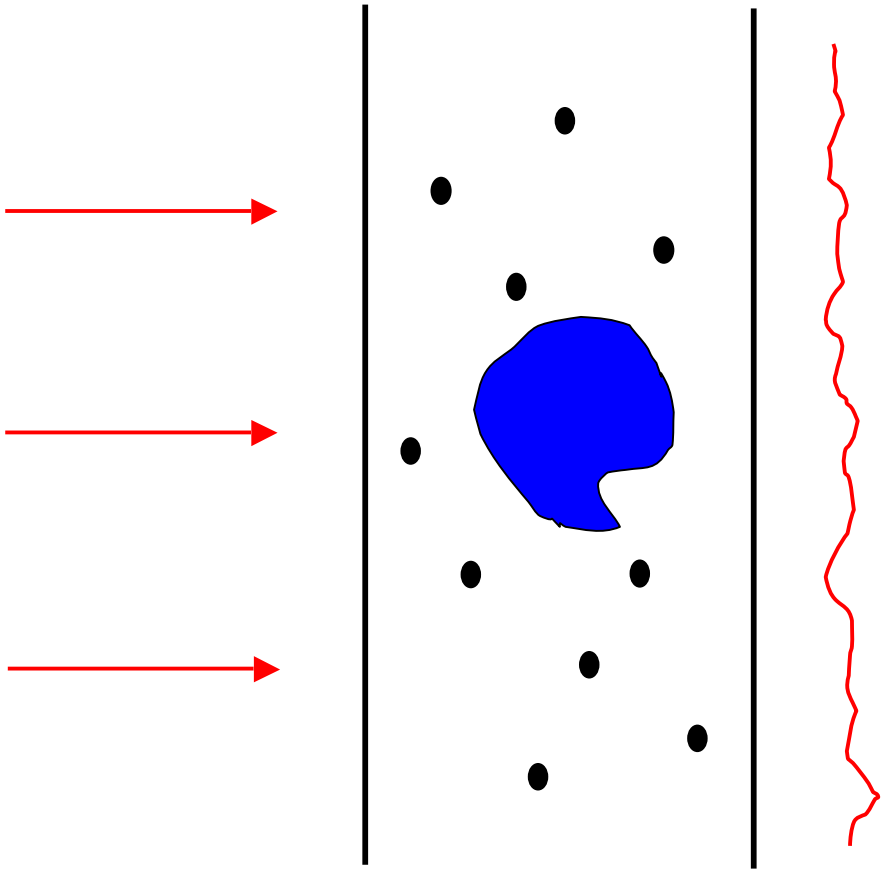

$L \gg \ell_s$

Inverse problem

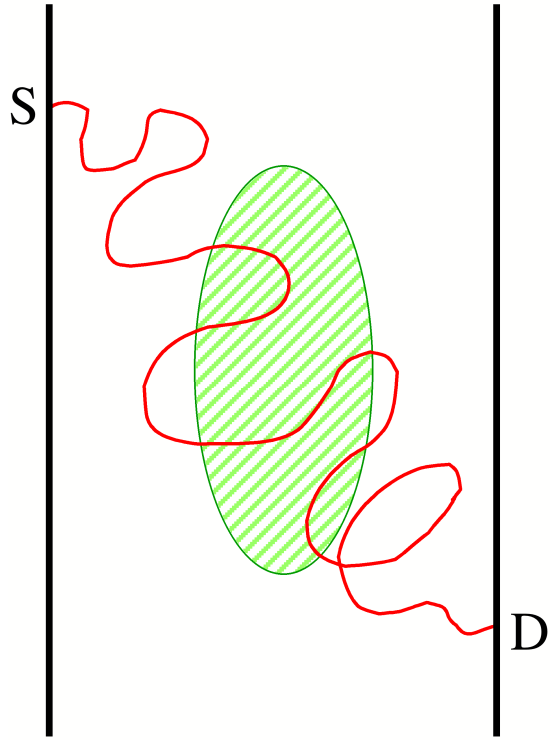

Problem: Reconstruct the optical absorption from boundary measurements.

Characteristic scales

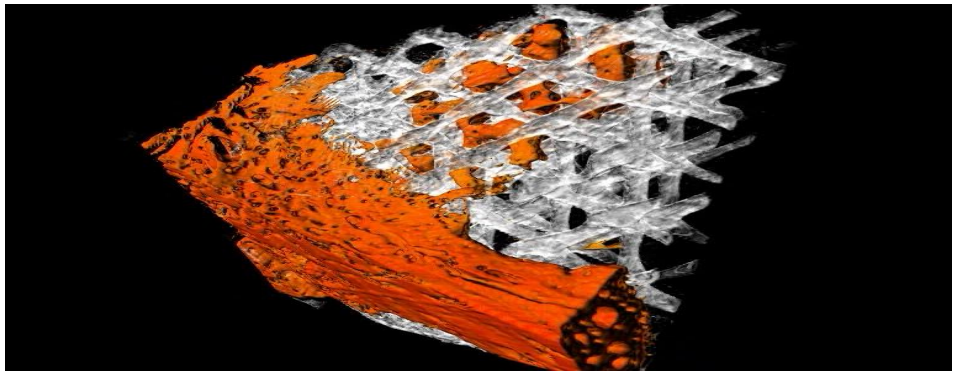

Microscopic ($L \ll \ell_s$)

Engineered tissue

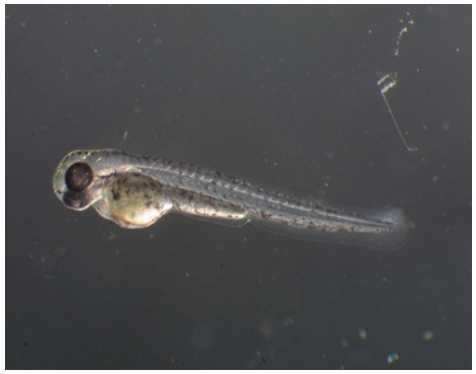

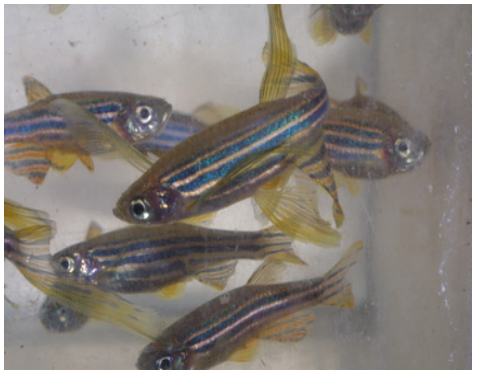

Mesoscopic ($L \sim \ell_s$)

Zebrafish embryo

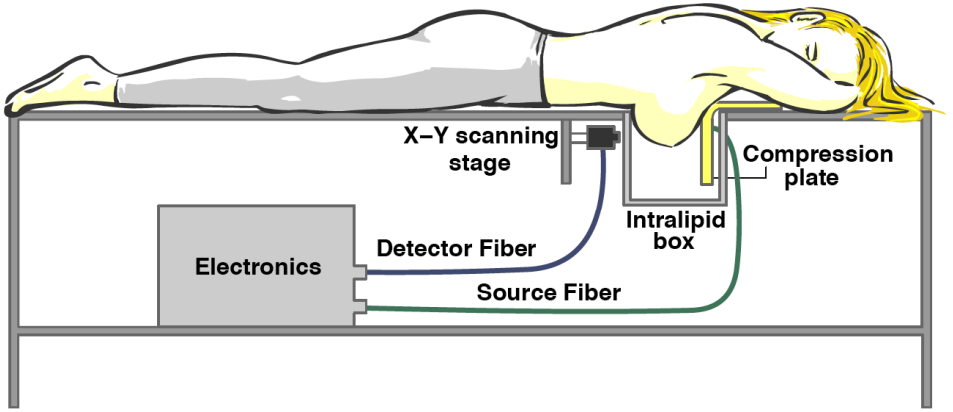

Macroscopic ($L \gg \ell_s$)

Human breast

Optical tomography

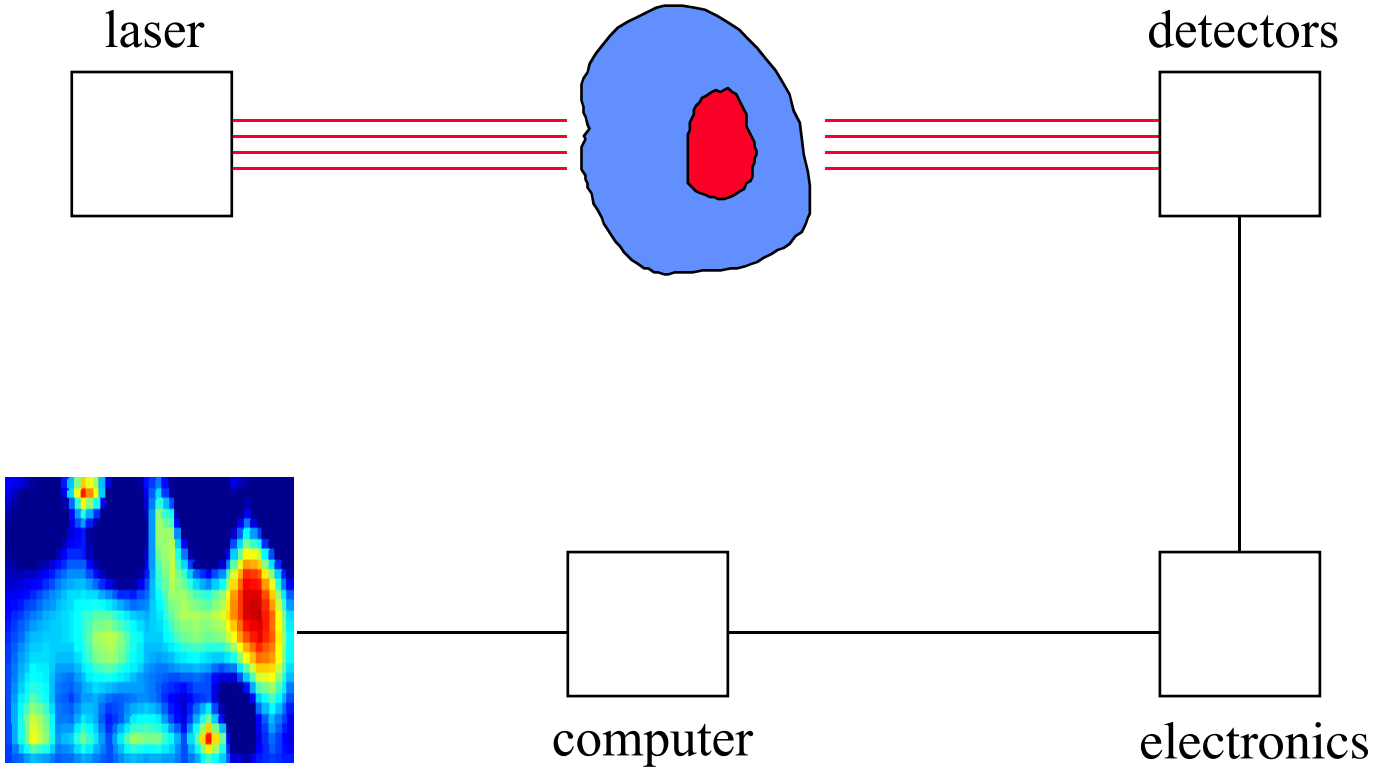

10^2 - 10^3 source detector pairs

Optical mammograms

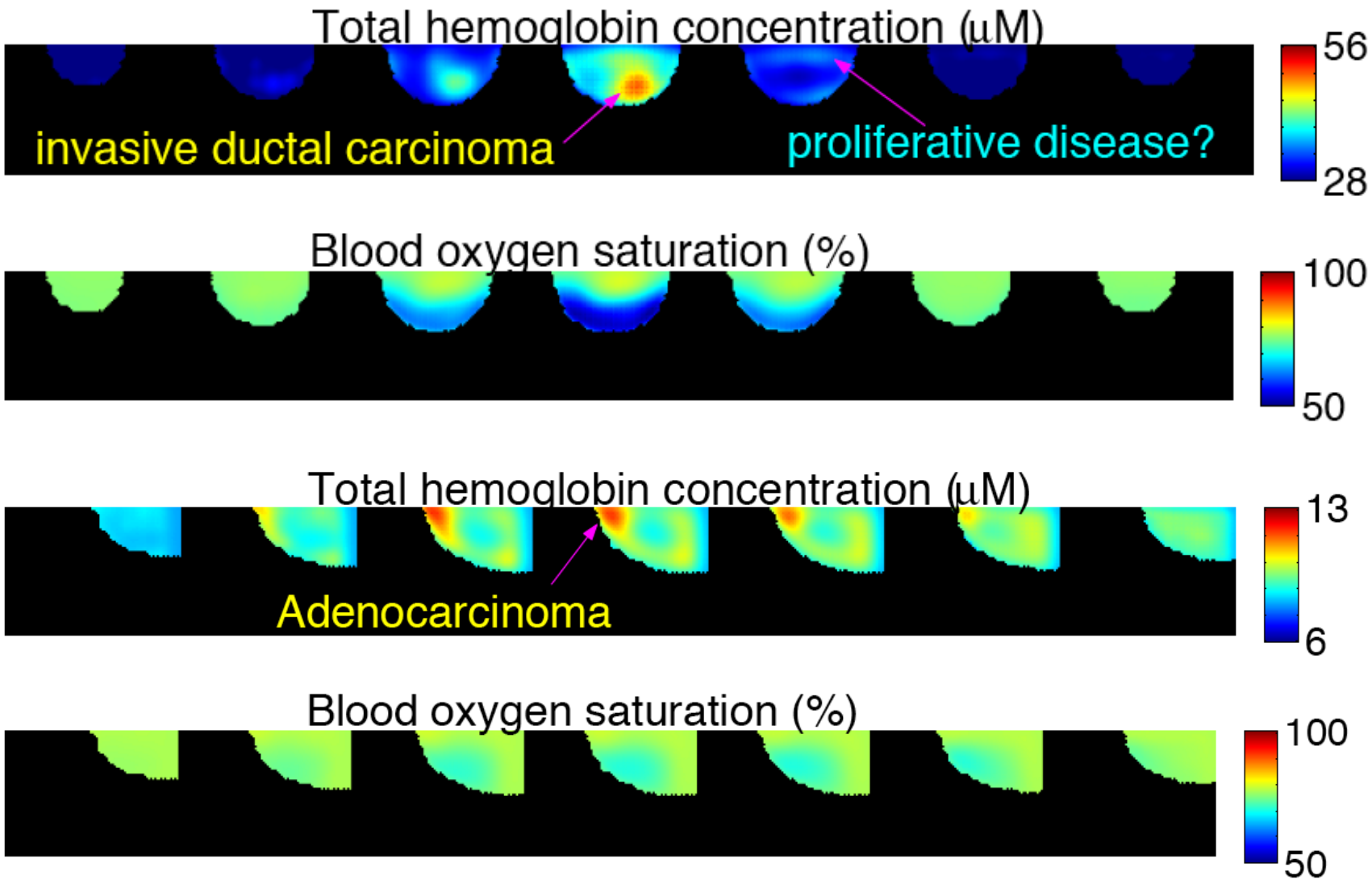

Choe and Yodh (2007)

Noncontact optical tomography (2005)

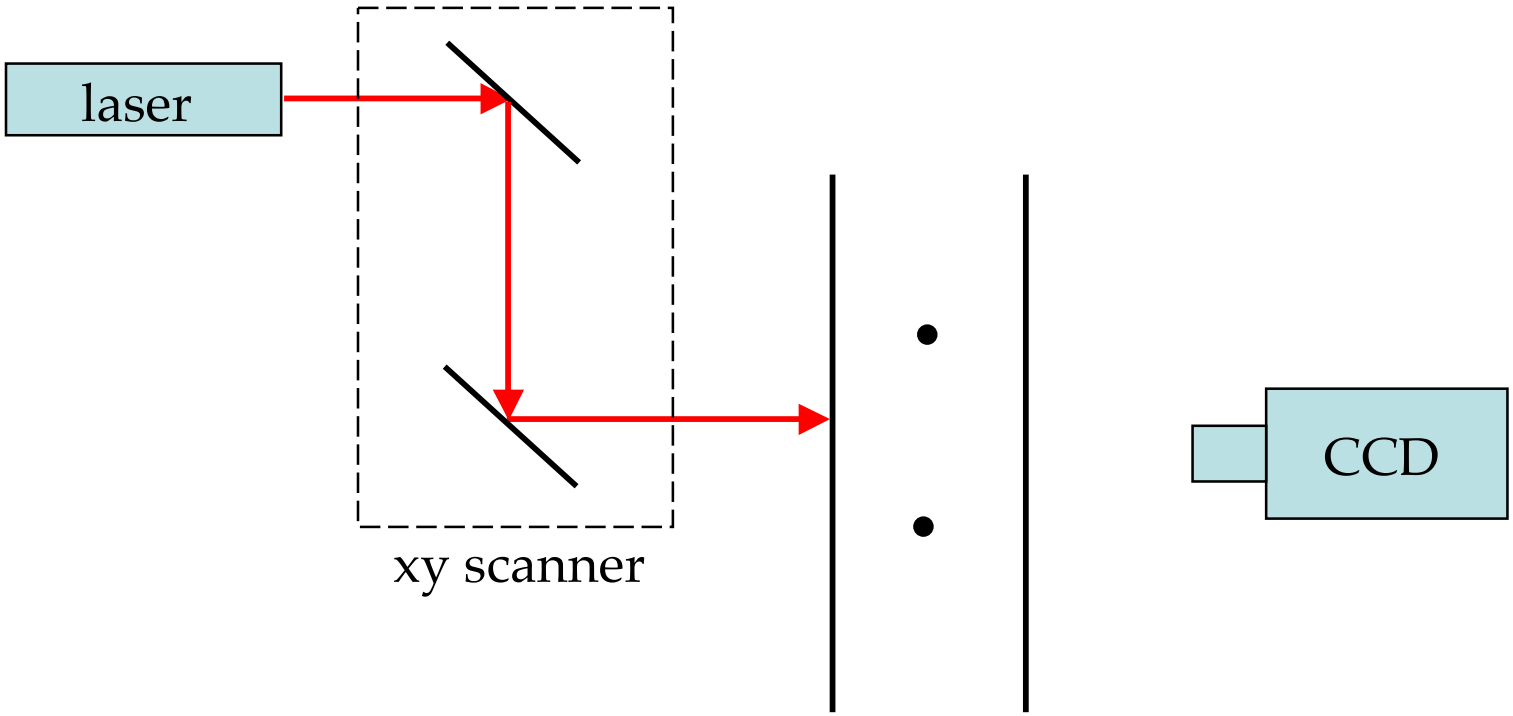

10^8 - 10^9 source detector pairs

Large data sets

- Access to higher spatial frequencies
  — increased resolution

- Fast Algorithms
  — $O(N)$ complexity
  — special geometries

Waves in random media

Transport of electromagnetic waves in random media is very familiar

- light propagation in fog, milk, biological tissue, interstellar media ...
- microscopic, mesoscopic and macroscopic descriptions

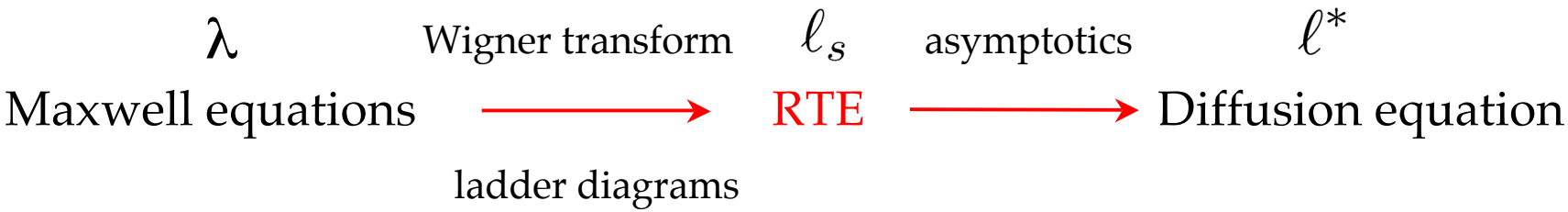

Waves ---------► Particles

Length scales

Consider a suspension of scatterers (paint, milk, tissue)

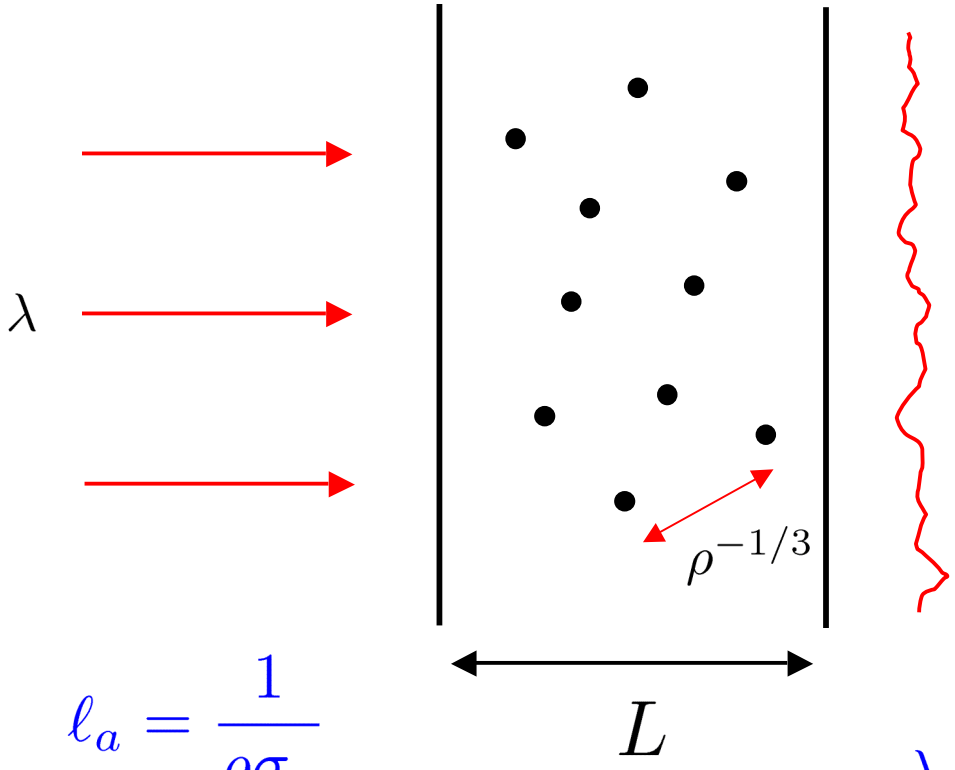

absorption cross section σ_a

scattering cross section σ_s

number density ρ

$$\ell_a = \frac{1}{\rho\sigma_a}$$

$$\ell_s = \frac{1}{\rho\sigma_s}$$

$\lambda \ll \ell_s \ll L, \ell_a$

$L \gg \ell_s$ multiple scattering

Radiative Transport Equation (RTE)

RTE describes conservation of specific intensity $I(\mathbf{r}, \hat{\mathbf{s}})$

$$\hat{\mathbf{s}} \cdot \nabla I + \mu_a I = \mu_s \int d^2 s' \left[p(\hat{\mathbf{s}}', \hat{\mathbf{s}}) I(\mathbf{r}, \hat{\mathbf{s}}') - p(\hat{\mathbf{s}}, \hat{\mathbf{s}}') I(\mathbf{r}, \hat{\mathbf{s}}) \right]$$

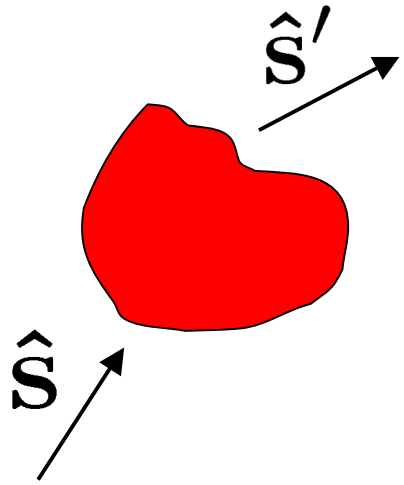

$\mu_a = 1/\ell_a$ is the absorption coefficient

$\mu_s = 1/\ell_s$ is the scattering coefficient

$p = \frac{d\sigma_s}{d\Omega} / \sigma_s$

RTE does not account for effects of interference and is not valid on the scale of the wavelength λ

No scattering ($\mu_s = 0$)

$$\hat{\mathbf{s}} \cdot \nabla I + \mu_a I = 0$$

$$I = I_0 \exp\left[- \int_L \mu_a dr \right] ,$$

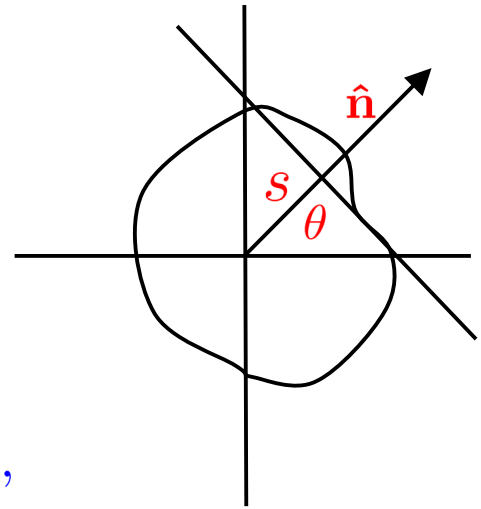

where $\hat{\mathbf{s}}$ is along the line L.

This exponential absorption law is the basis for CT.

Thus we can measure the 2D Radon transform

$$Rf(\hat{\mathbf{n}}, s) = \int f(\mathbf{r}) \delta(\hat{\mathbf{n}} \cdot \mathbf{r} - s) d^2 r ,$$

which can be inverted

$$f(\mathbf{r}) = \frac{1}{2\pi^2} \int_0^\pi d\theta \int_{-\infty}^{\infty} ds \frac{1}{\hat{\mathbf{n}}(\theta) \cdot \mathbf{r} - s} \frac{\partial}{\partial s} Rf(\hat{\mathbf{n}}(\theta), s) .$$

Characteristic scales

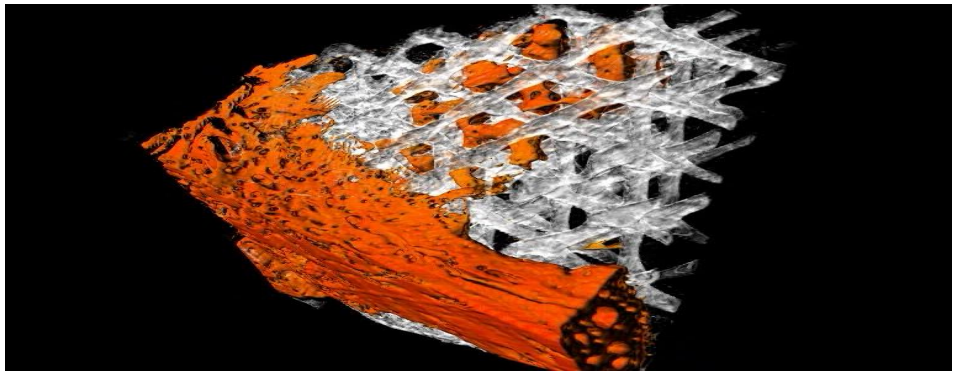

Microscopic ($L \ll \ell_s$)

Engineered tissue

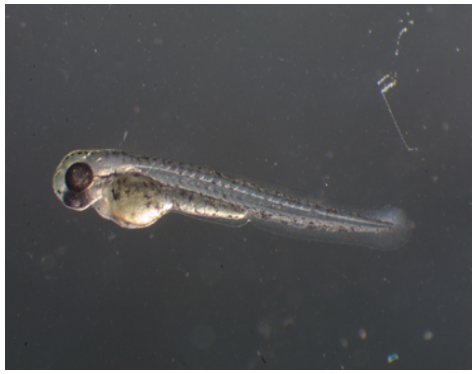

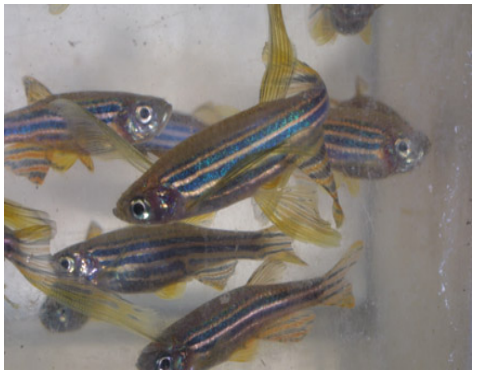

Mesoscopic ($L \sim \ell_s$)

Zebrafish embryo

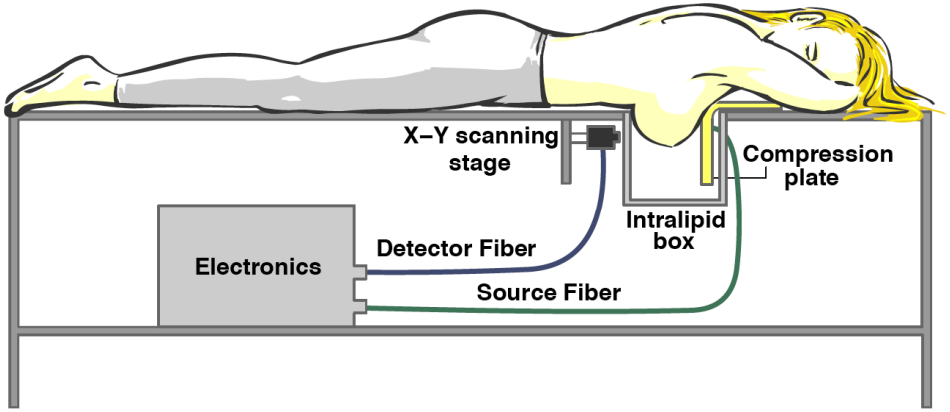

Macroscopic ($L \gg \ell_s$)

Human breast

Single-scattering regime

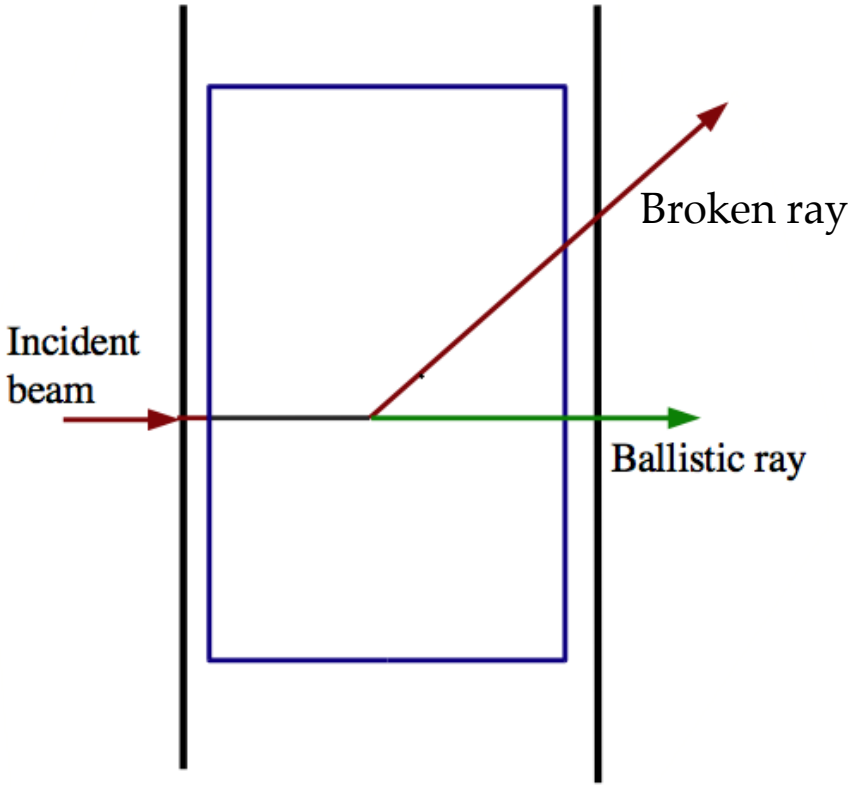

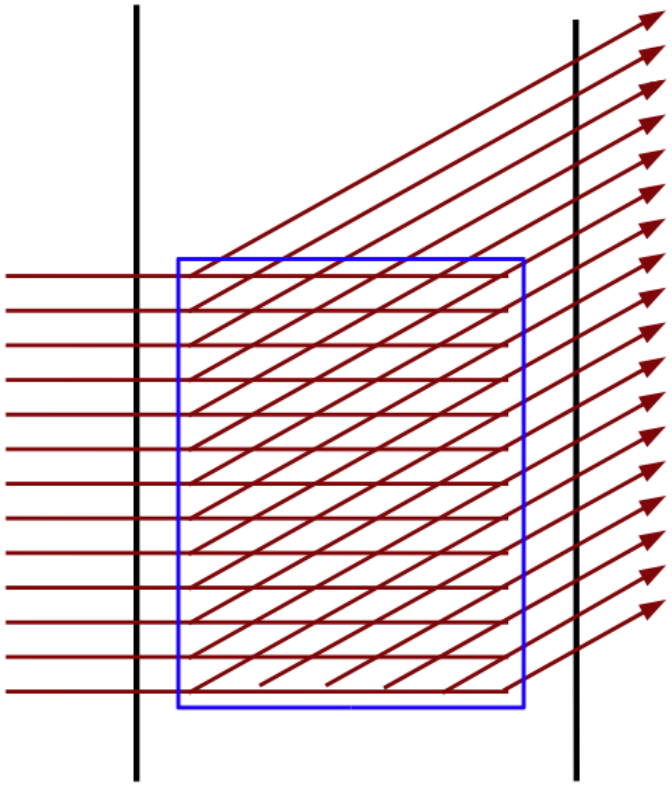

Collision expansion

Consider the RTE

$$[\hat{\mathbf{s}} \cdot \nabla + \mu_a(\mathbf{r}) + \mu_s(\mathbf{r})] I(\mathbf{r}, \hat{\mathbf{s}}) = \mu_s(\mathbf{r}) \int p(\hat{\mathbf{s}}, \hat{\mathbf{s}}') I(\mathbf{r}, \hat{\mathbf{s}}') d^2 s'$$

The solution is given by

$$I(\mathbf{r}, \hat{\mathbf{s}}) = I_0(\mathbf{r}, \hat{\mathbf{s}}) + \int d^3 r' d^2 s' d^2 s'' G(\mathbf{r}, \hat{\mathbf{s}}; \mathbf{r}', \hat{\mathbf{s}}') p(\hat{\mathbf{s}}', \hat{\mathbf{s}}'') \mu_s(\mathbf{r}') I(\mathbf{r}', \hat{\mathbf{s}}'') \, ,$$

where G is the ballistic Green's function for the RTE with $\mu_s = 0$.

Collision expansion

Single-scattering

Within the accuracy of the single-scattering approximation, the change in specific intensity produced by a unidirectional point source is given by

$$\Delta I(\mathbf{r}_1, \hat{\mathbf{s}}_1; \mathbf{r}_2, \hat{\mathbf{s}}_2) = \int d^3r d^2s d^2s' G(\mathbf{r}_2, \hat{\mathbf{s}}_2; \mathbf{r}, \hat{\mathbf{s}}) G(\mathbf{r}, \hat{\mathbf{s}}; \mathbf{r}_1, \hat{\mathbf{s}}_1) p(\hat{\mathbf{s}}, \hat{\mathbf{s}}') \mu_s(\mathbf{r}') \; .$$

The ballistic Green's function G is

$$G(\mathbf{r}, \hat{\mathbf{s}}; \mathbf{r}', \hat{\mathbf{s}}') = g(\mathbf{r}, \mathbf{r}') \delta(\hat{\mathbf{s}} - \hat{\mathbf{s}}') \delta \left(\frac{\mathbf{r} - \mathbf{r}'}{|\mathbf{r} - \mathbf{r}'|} - \hat{\mathbf{s}}' \right) \; ,$$

where

$$g(\mathbf{r}, \mathbf{r}') = \frac{1}{|\mathbf{r} - \mathbf{r}'|^2} \exp \left[- \int_0^{|\mathbf{r} - \mathbf{r}'|} \mu_t \left(\mathbf{r}' + \ell \frac{\mathbf{r} - \mathbf{r}'}{|\mathbf{r} - \mathbf{r}'|} \right) d\ell \right]$$

and $\mu_t = \mu_a + \mu_s$.

$I \; =$ 

Measurable quantities

Accounting only for single scattering, ΔI is given by

$$\Delta I(\mathbf{r}_1, \hat{\mathbf{s}}_1; \mathbf{r}_2, \hat{\mathbf{s}}_2) = \delta(|\varphi_1 - \varphi_2| - \pi) \frac{p(\hat{\mathbf{s}}_1, \hat{\mathbf{s}}_2)\mu_s(\mathbf{R})}{r_{21} \sin\vartheta_1 \sin\vartheta_2}$$

$$\times \exp\left[- \int_0^{L_1} \mu_t(\mathbf{r}_1 + \ell\hat{\mathbf{s}}_1) d\ell - \int_0^{L_2} \mu_t(\mathbf{R} + \ell\hat{\mathbf{s}}_2) d\ell \right] ,$$

where $\varphi_{1,2}$ are the azimuthal angles of $\hat{\mathbf{s}}_{1,2}$ in a coordinate system whose z axis lies along $\mathbf{r}_{21}$. In an experiment, the observable quantity is the angular integral of the intensity over an aperture. Thus, the integral of μ_t along a broken ray is directly measurable.

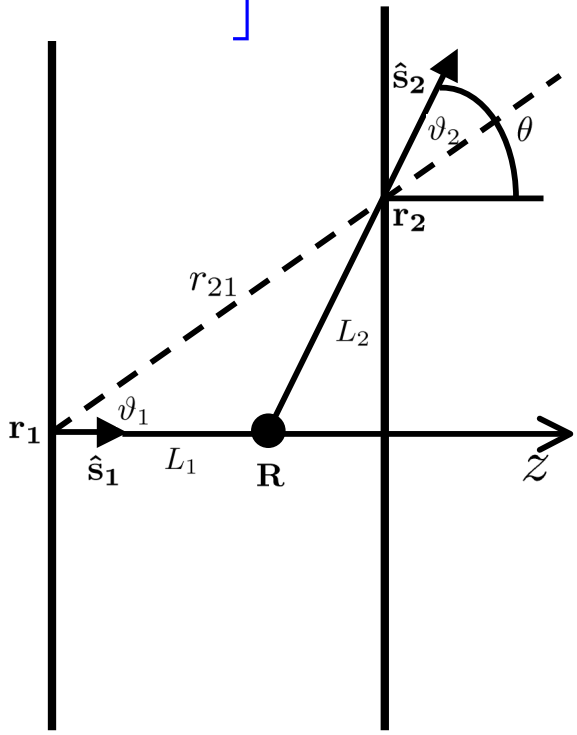

Broken-ray Radon transform

Let f be a sufficiently smooth function with compact support in the slab. The broken-ray Radon transform is defined by

$$R_b f(\mathbf{r}_1, \hat{\mathbf{s}}_1; \mathbf{r}_2, \hat{\mathbf{s}}_2) = \int_{BR(\mathbf{r}_1, \hat{\mathbf{s}}_1; \mathbf{r}_2, \hat{\mathbf{s}}_2)} f\, dx \ ,$$

where $BR(\mathbf{r}_1, \hat{\mathbf{s}}_1; \mathbf{r}_2, \hat{\mathbf{s}}_2)$ denotes the broken ray which begins at $\mathbf{r}_1$, travels in the direction $\hat{\mathbf{s}}_1$ and ends at $\mathbf{r}_2$ in the direction $\hat{\mathbf{s}}_2$.

If $\mathbf{r}_1, \mathbf{r}_2, \hat{\mathbf{s}}_1$ and $\hat{\mathbf{s}}_2$ all lie in the same plane, then the point of intersection $\mathbf{R}$ is uniquely determined. It will suffice to consider the inverse problem in the plane and to reconstruct the function f from two-dimensional slices. Note that when $\hat{\mathbf{s}}_1 = \hat{\mathbf{s}}_2 = \hat{\mathbf{r}}_{12}$, R_b reduces to the two-dimensional Radon transform.

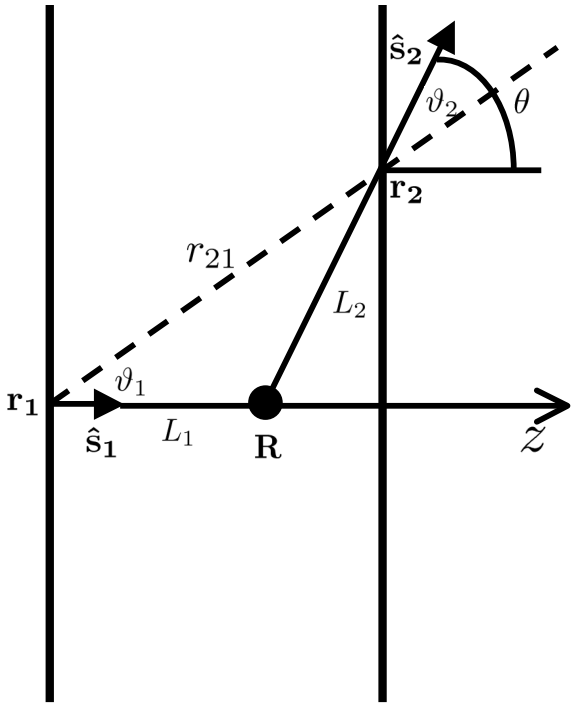

Inversion formula I

The problem of inverting R_b is overdetermined. However, if the directions $\hat{\mathbf{s}}_1$ and $\hat{\mathbf{s}}_2$ are taken to be fixed, then the inverse problem is formally determined. In the slab geometry

$$R_b f(y_1, y_2) = \int_0^{L_1} f(y_1, z) dz + \sec\theta \int_{L_1}^{L} f\left((z - L)\tan\theta + y_2, z\right) dz \; .$$

An inversion formula can be derived by making use of the translational invariance of the slab in the source plane and introducing the Fourier transform $\tilde{f}(k, z)$ of $f(y, z)$ with respect to y. It can then be shown that $\tilde{f}$ obeys a one-dimensional integral equation which can be solved explicitly.

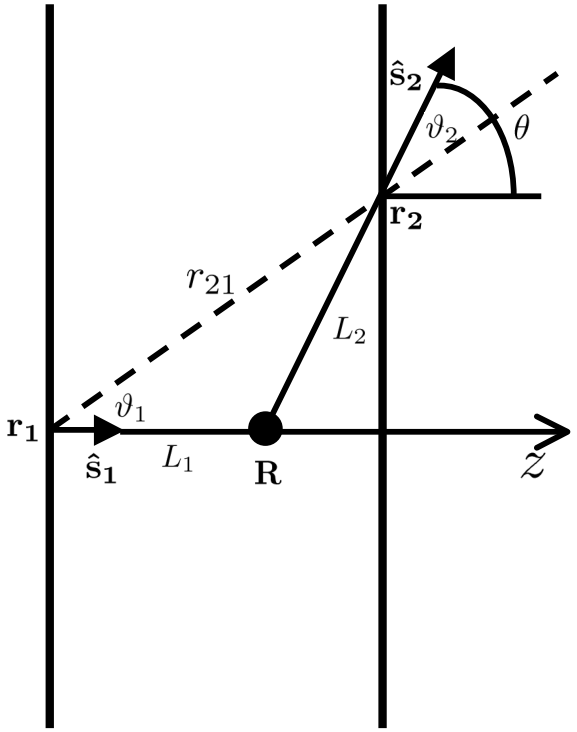

Inversion formula II

The inversion formula for R_b is

$$\begin{aligned} f(y,z) &= \lambda \left\{ \left[\frac{\partial}{\partial \Delta} - (1+\kappa)\frac{\partial}{\partial y} \right] \psi(y,\Delta) + \kappa \frac{\partial}{\partial y} \psi(y+\lambda z, \Delta_{\max}) \right. \\ &- \left. \kappa(1+\kappa)\frac{\partial^2}{\partial y^2} \int_{\Delta}^{\Delta_{\max}} \psi\Big(y+\kappa(\ell-\Delta),\ell\Big) d\ell \right\} \Bigg|_{\Delta=(L-z)\tan\theta}, \end{aligned}$$

where $\Delta_{\max} = L\tan\theta$, $\lambda = \cot(\theta/2)$ and $\kappa = \cot(\theta/2)\cot\theta$.

Remarks

- In contrast to computed tomography, it is unnecessary to collect projections along rays which are rotated about the sample.
- It is possible to derive an inversion formula in the backscattering geometry in which the sources and detectors are located on the same plane.

Reconstructions

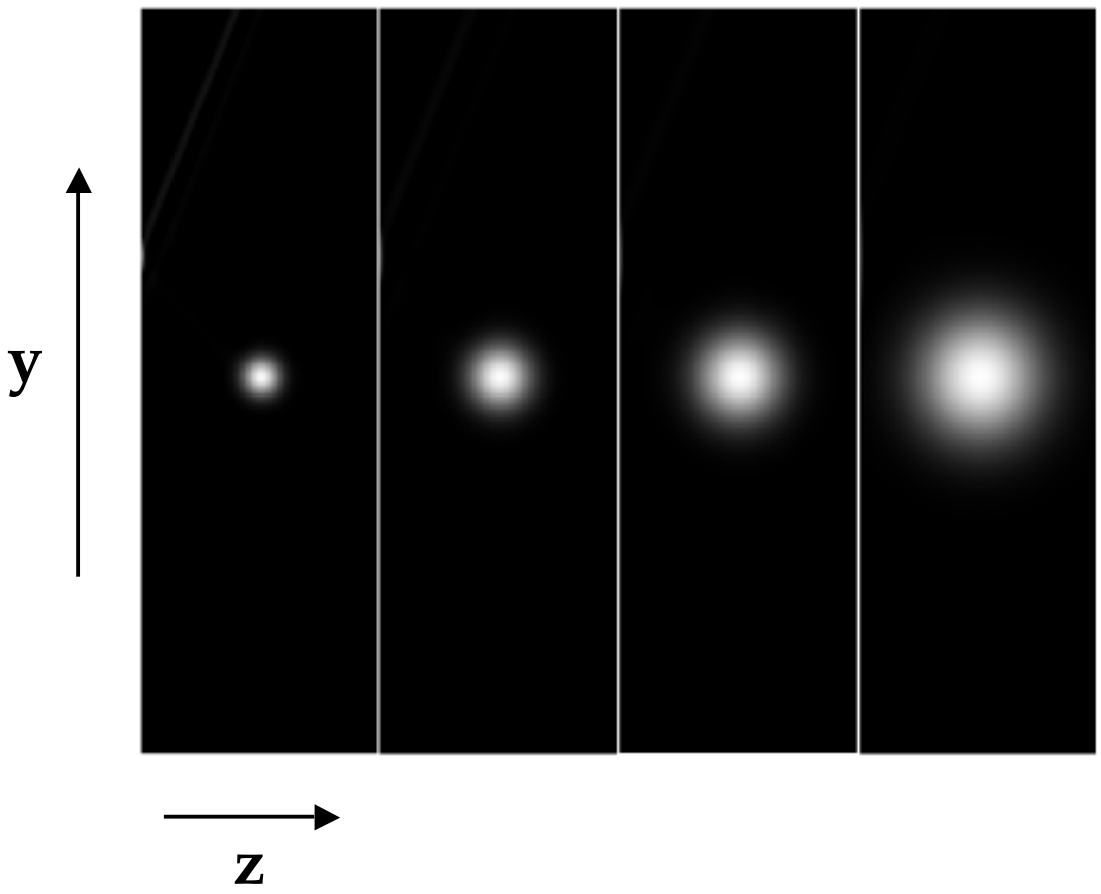

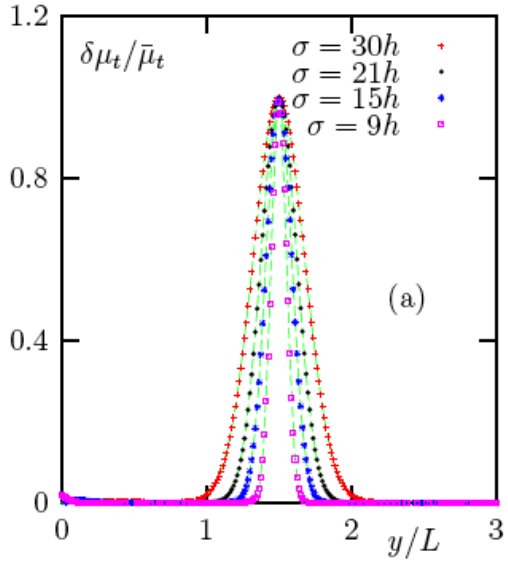

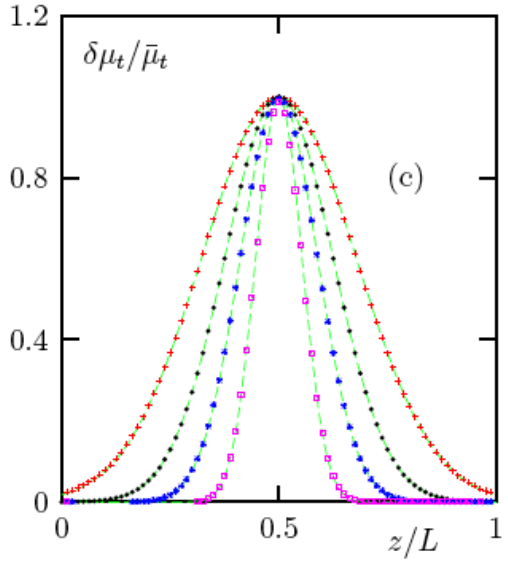

Characteristic scales

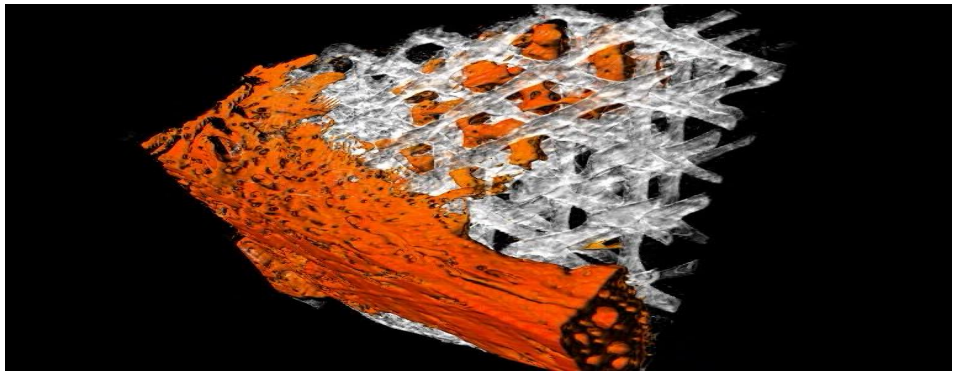

Microscopic ($L \ll \ell$)

Engineered tissue

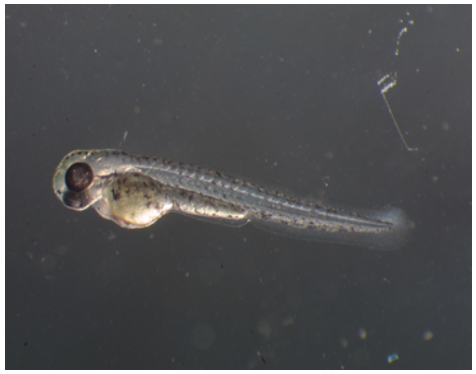

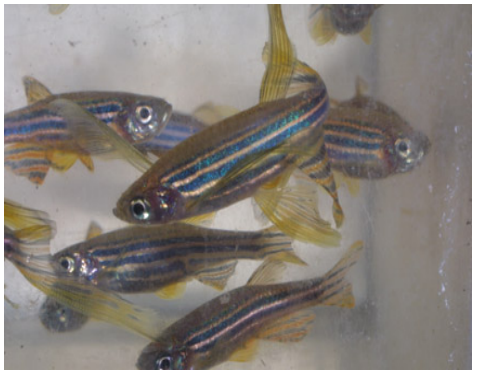

Mesoscopic ($L \sim \ell$)

Zebrafish embryo

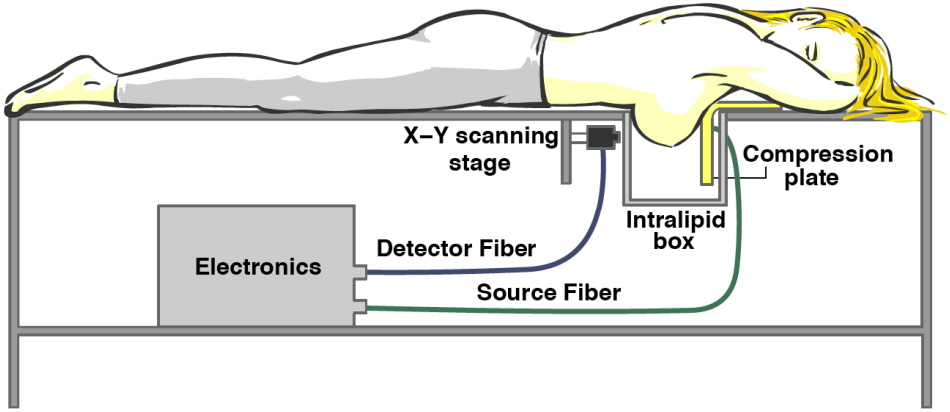

Macroscopic ($L \gg \ell$)

Human breast

Scattering theory for the RTE

Consider an inhomogeneous absorbing medium with $\mu_a = \mu_a^0 + \delta\mu_a$.

$$I(\mathbf{r}, \hat{\mathbf{s}}) = I_{\text{in}}(\mathbf{r}, \hat{\mathbf{s}}) - \int d^3r' d^2s' G(\mathbf{r}, \hat{\mathbf{s}}; \mathbf{r}', \hat{\mathbf{s}}') \delta\mu_a(\mathbf{r}') I(\mathbf{r}', \hat{\mathbf{s}}')$$

G is the Green's function for the RTE with $\mu_a = \mu_a^0$

The linearization of the above integral equation with respect to $\delta\mu_a$ is given by

$$\phi(\mathbf{r}_1, \hat{\mathbf{s}}_1; \mathbf{r}_2, \hat{\mathbf{s}}_2) = \int d^3r d^2s G(\mathbf{r}_1, \hat{\mathbf{s}}_1; \mathbf{r}, \hat{\mathbf{s}}) G(\mathbf{r}, \hat{\mathbf{s}}; \mathbf{r}_2, \hat{\mathbf{s}}_2) \delta\mu_a(\mathbf{r}) \, ,$$

where $\phi = I_{\text{in}} - I$. The approximation is accurate if $\delta\mu_a$ is small and $\text{supp}(\delta\mu_{\text{a}})$ is small.

Exact solutions to the RTE

There are very few exact solutions to the RTE. The Green's function is known analytically for only the following cases:

- Isotropic scattering in three dimensions without boundaries
- Isotropic scattering in one dimension with planar boundaries
- Approximate methods
  — diffusion approximation
  — P_l approximation

Diffusion approximation

The diffusion approximation arises from accounting for the lowest-order angular dependence of the Green's function for the RTE. That is

$$G(\mathbf{r},\hat{\mathbf{s}};\mathbf{r}',\hat{\mathbf{s}}') = \frac{c}{4\pi}\left(1+\ell^*\hat{\mathbf{s}}\cdot\nabla_{\mathbf{r}}\right)\left(1-\ell^*\hat{\mathbf{s}}\cdot\nabla_{\mathbf{r}'}\right)G(\mathbf{r},\mathbf{r}')\ ,$$

where $G(\mathbf{r},\mathbf{r}')$ is the diffusion Green's function which obeys

$$\left(-D_0\nabla^2+c\mu_a^0\right)G(\mathbf{r},\mathbf{r}') = \delta(\mathbf{r}-\mathbf{r}')$$

The DA is accurate when $\ell^*|\nabla G| \ll G$, that is when the intensity varies slowly on the scale of ℓ^*. This condition breaks down in thin layers, with weak scattering and near boundaries.

Diffusion approximation

Consider the integral equation

$$\phi(\mathbf{r}_1, \hat{\mathbf{s}}_1; \mathbf{r}_2, \hat{\mathbf{s}}_2) = \int d^3r d^2s G(\mathbf{r}_1, \hat{\mathbf{s}}_1; \mathbf{r}, \hat{\mathbf{s}}) G(\mathbf{r}, \hat{\mathbf{s}}; \mathbf{r}_2, \hat{\mathbf{s}}_2) \delta\mu_a(\mathbf{r}) \; .$$

Within the accuracy of the DA, ϕ is given by

$$\phi(\mathbf{r}_1, -\hat{\mathbf{n}}; \mathbf{r}_2, \hat{\mathbf{n}}) = \int d^3r G(\mathbf{r}_1, \mathbf{r}) G(\mathbf{r}, \mathbf{r}_2) \delta\alpha(\mathbf{r})$$

where $\delta\alpha = c\delta\mu_a$ and $G(\mathbf{r}, \mathbf{r}')$ is the Green's function for the RTE within the DA.

Diffusion Green's function

$$G(\mathbf{r},\mathbf{r}') = \int \frac{d^2q}{(2\pi)^2} e^{i\mathbf{q}\cdot(\boldsymbol{\rho}-\boldsymbol{\rho}')} g(\mathbf{q};z,z')$$

with $\mathbf{r} = (\boldsymbol{\rho}, z)$.

Infinite medium

$g(\mathbf{q};z,z') = \frac{1}{2Q(q)D} \exp[-Q(q)|z-z'|]$

Semi-infinite medium

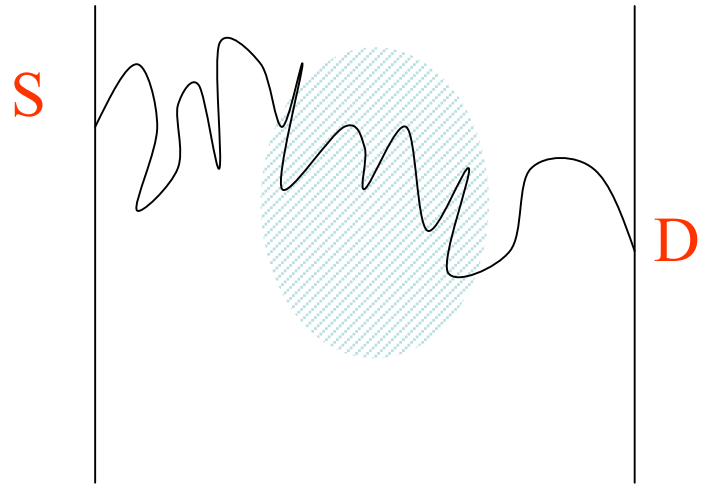

$$g(\mathbf{q};z,z') = \frac{1}{2Q(q)D}\left[\frac{Q(q)\ell - 1}{Q(q)\ell + 1}\exp\left(-Q(q)|z+z'|\right) + \exp\left(-Q(q)|z-z'|\right)\right]$$

with $Q(q) = \sqrt{q^2+k^2}$. Here $k = \sqrt{3\mu_a\mu_s'} \approx 1\text{cm}^{-1}$

Inverse problem

The forward problem of optical tomography is to compute the scattering data ϕ from the absorption $\delta\alpha$. The inverse problem is to recover $\delta\alpha$ from ϕ. The simplest approach is to solve the integral equation

$$\phi_B(\mathbf{r}_1, \mathbf{r}_2) = \int G(\mathbf{r}_1, \mathbf{r}) G(\mathbf{r}, \mathbf{r}_2) \delta\alpha(\mathbf{r}) d^3 r$$

by a numerical method. This approach is computationally expensive and not suitable for use with large data sets.

Instead, we make use of a direct method (invesion formula).

Fourier-Laplace structure of the DA

Recall the linearized integral equation in the diffusion approximation

$$\phi(\mathbf{r}_1, \mathbf{r}_2) = \int d^3 r G(\mathbf{r}_1, \mathbf{r}) G(\mathbf{r}, \mathbf{r}_2) \delta\alpha(\mathbf{r})$$

It can be seen that the Fourier transform of ϕ is given by

$$\widetilde{\phi}(\mathbf{q}_1, \mathbf{q}_2) = \int d^3 r \exp[i(\mathbf{q}_1 - \mathbf{q}_2) \cdot \boldsymbol{\rho} - (Q(\mathbf{q}_1) + Q(\mathbf{q}_2))z] \delta\alpha(\mathbf{r})$$

- ISP is exponentially ill-posed in depth direction
- ISP is well-posed in transverse direction
- Transverse resolution determined by the highest spatial frequencies in the measurements. Implications for large data sets

Noncontact imager

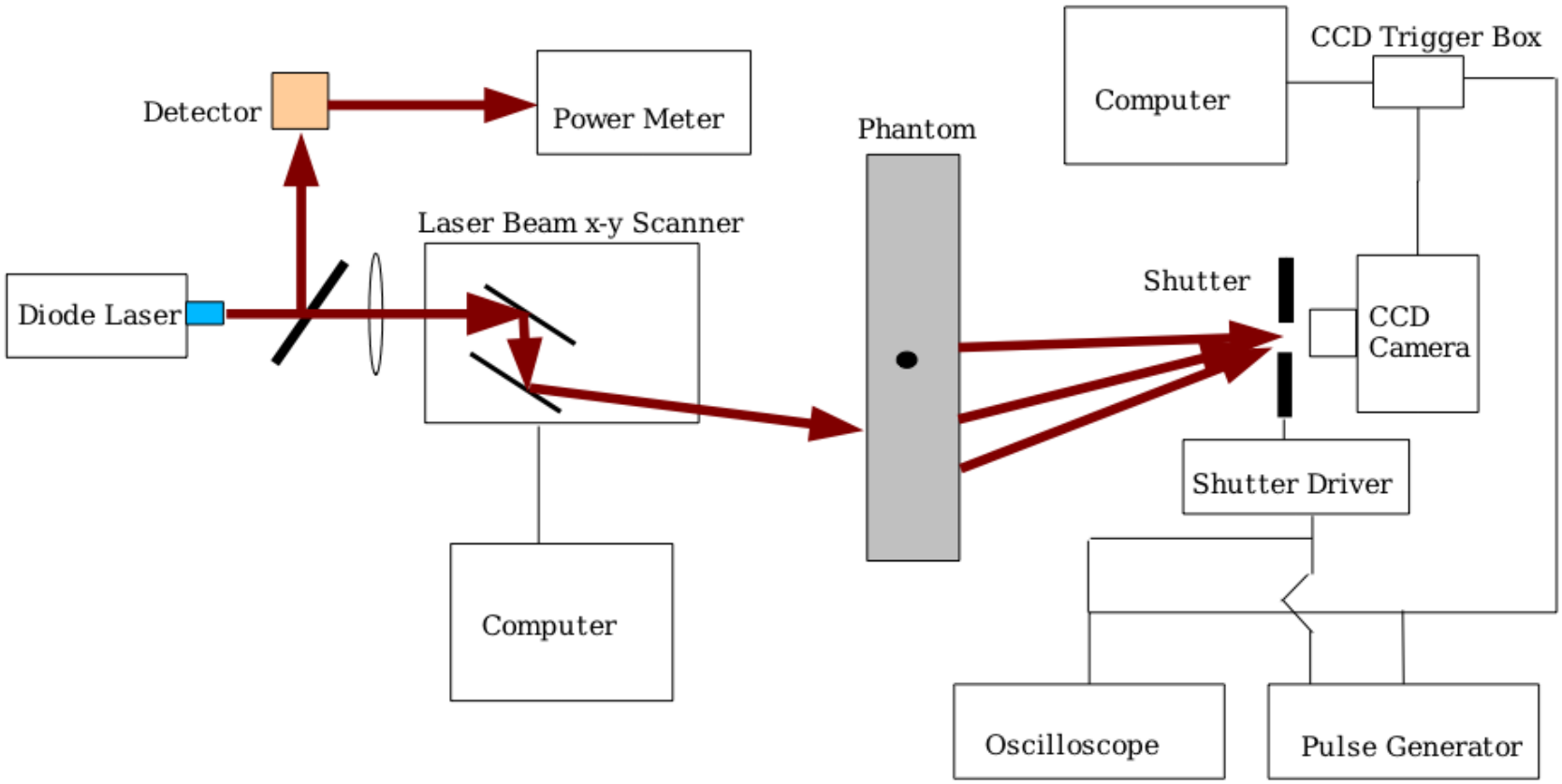

Transmission through a slab

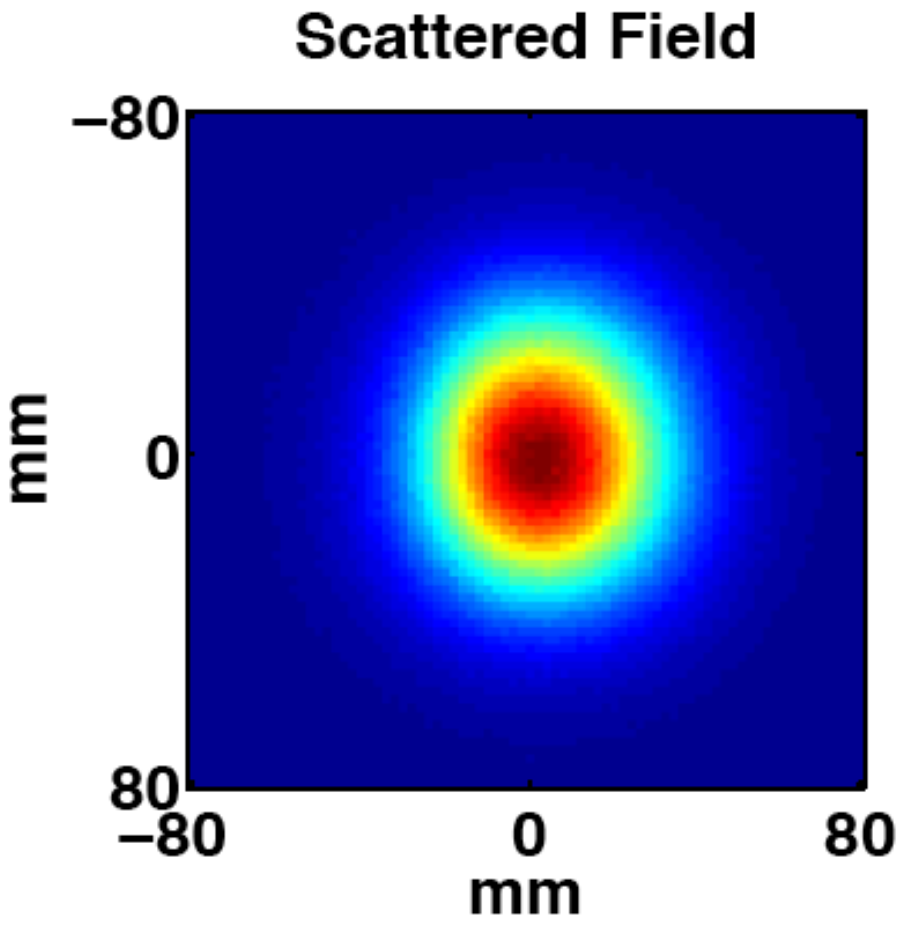

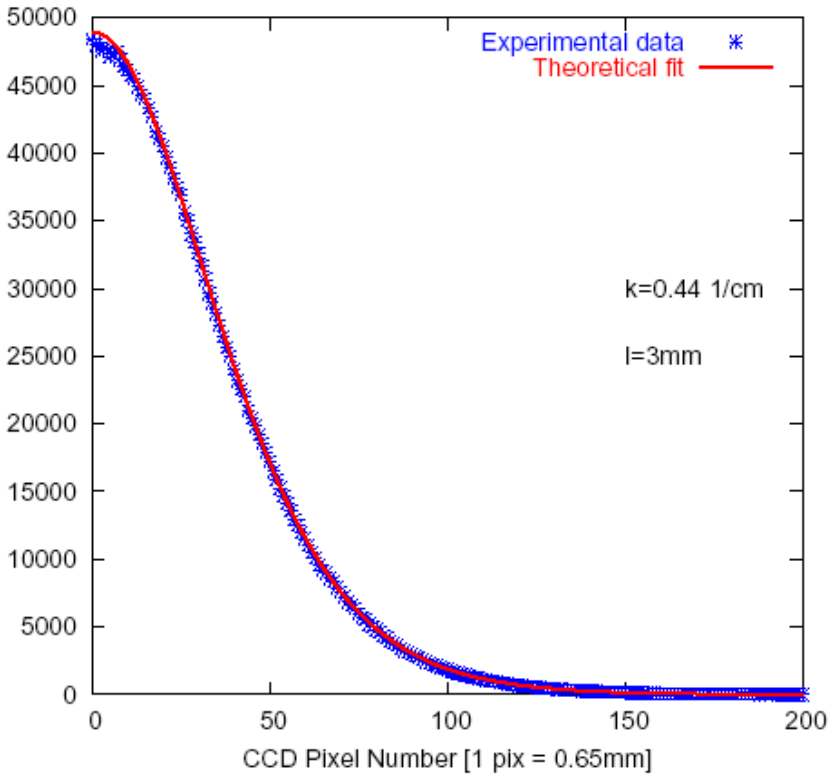

Reconstructions from experimental data

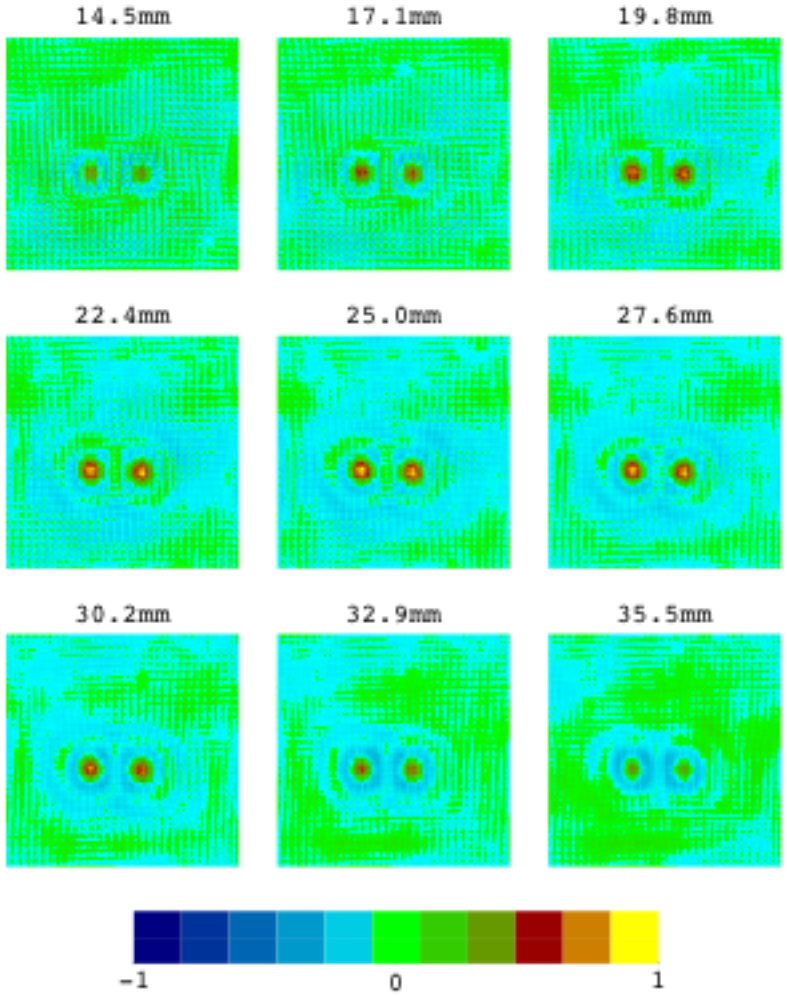

- 10^8 source-detector pairs
- 10^3 sources and 10^5 detectors
- 8 mm diameter black balls in 1% IL
- Balls in midplane of slab
- 50 mm slab thickness
- 2.6 mm slice separation
- 256 $\times$ 256 pixels per slice
- 15 cm $\times$ 15 cm FOV
- Reconstruction time ~ 10 min

Resolution and bar targets

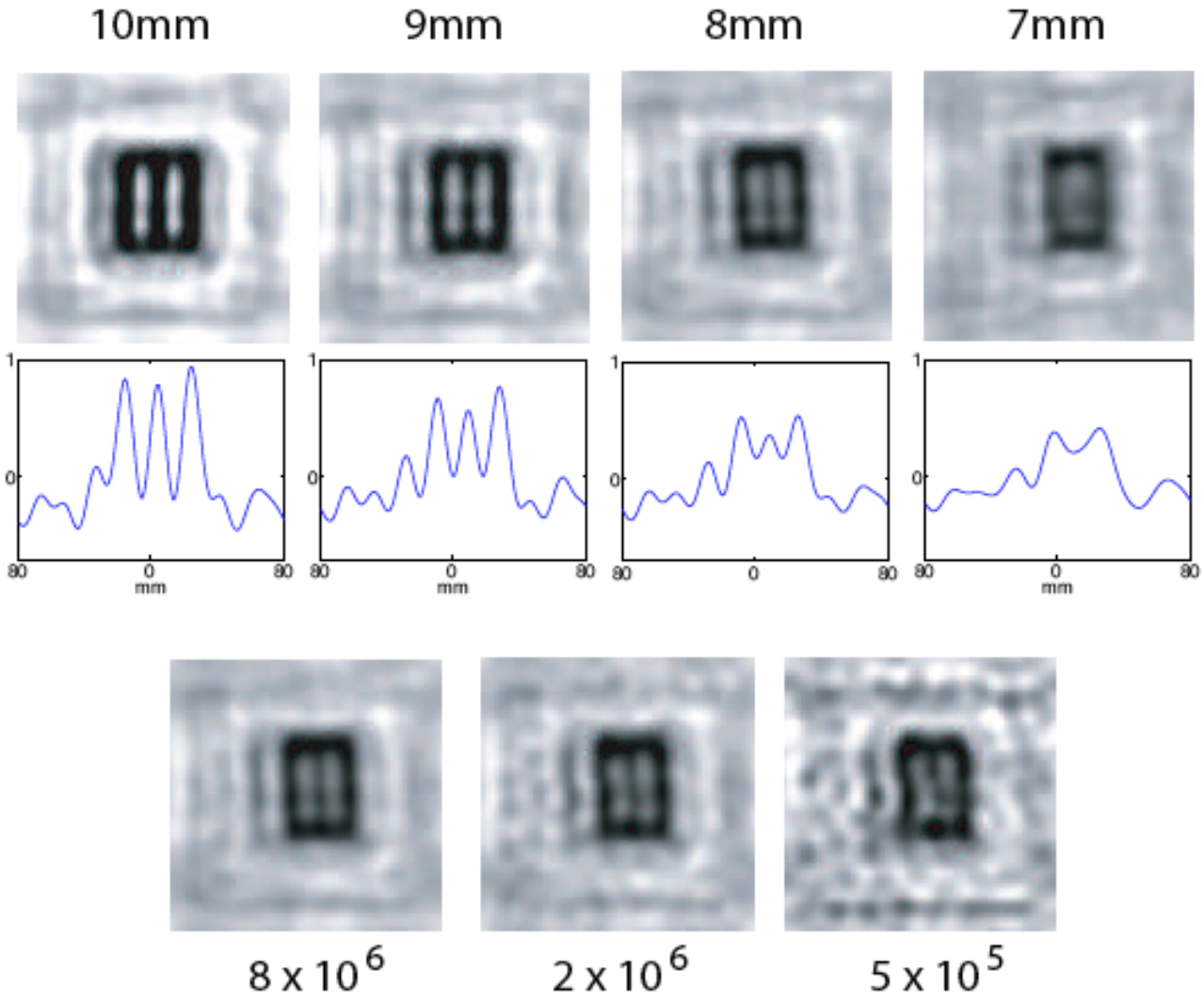

Reconstruction of shape

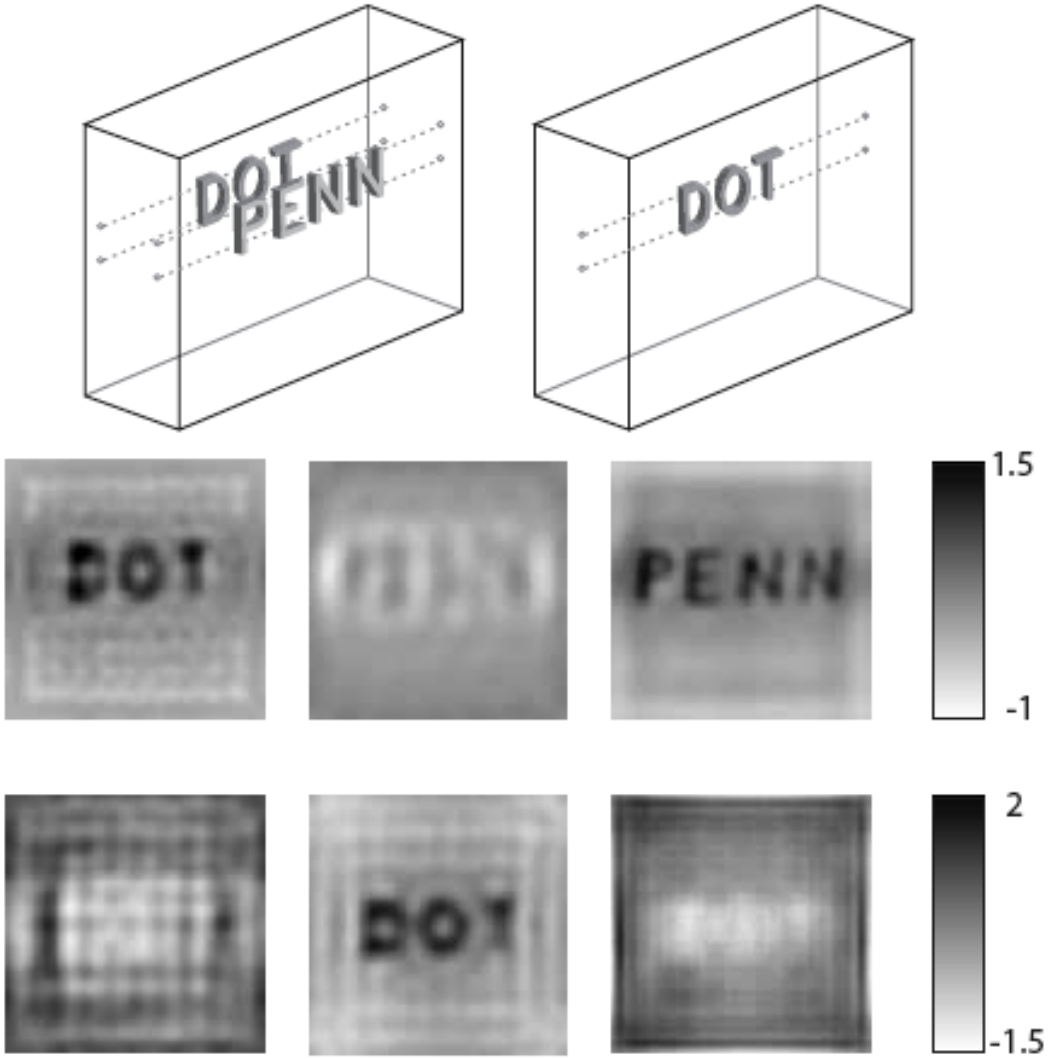

4×10^7 source-detector pairs

6 cm slab thickness

Letters are 3 mm wide

3:1 absorption contrast

FOV = 12 cm x 12 cm

Reconstruction time $\approx$ 1 min

Breakdown of diffusion approximation

- Optically thin samples
- Weakly scattering media
- Strongly absorbing media
- Boundary layers

Scattering theory for the RTE

Consider an inhomogeneous absorbing medium with $\mu_a = \mu_a^0 + \delta\mu_a$.

$$I(\mathbf{r}, \hat{\mathbf{s}}) = I_{\text{in}}(\mathbf{r}, \hat{\mathbf{s}}) - \int d^3r' d^2s' G(\mathbf{r}, \hat{\mathbf{s}}; \mathbf{r}', \hat{\mathbf{s}}') \delta\mu_a(\mathbf{r}') I(\mathbf{r}', \hat{\mathbf{s}}')$$

G is the Green's function for the RTE with $\mu_a = \mu_a^0$

The linearization of the above integral equation with respect to $\delta\mu_a$ is given by

$$\phi(\mathbf{r}_1, \hat{\mathbf{s}}_1; \mathbf{r}_2, \hat{\mathbf{s}}_2) = \int d^3r d^2s G(\mathbf{r}_1, \hat{\mathbf{s}}_1; \mathbf{r}, \hat{\mathbf{s}}) G(\mathbf{r}, \hat{\mathbf{s}}; \mathbf{r}_2, \hat{\mathbf{s}}_2) \delta\mu_a(\mathbf{r}) \, ,$$

where $\phi = I_{\text{in}} - I$. The approximation is accurate if $\delta\mu_a$ is small and $\text{supp}(\delta\mu_{\text{a}})$ is small.

Evanescent modes for the RTE I

We look for evanescent modes of the form $I(\mathbf{r}, \hat{\mathbf{s}}) = A(\hat{\mathbf{s}})e^{\mathbf{k}\cdot\mathbf{r}}$, where $\mathbf{k} = i\mathbf{q} \pm \sqrt{q^2 + 1/\lambda^2}\,\hat{\mathbf{z}}$ and $\mathbf{k}\cdot\mathbf{k} = 1/\lambda^2$. These are the analogs of diffuse modes or complex geometrical optics solutions.

$$\left(\hat{\mathbf{s}}\cdot\hat{\mathbf{k}} + \mu_a + \mu_s\right) A(\hat{\mathbf{s}}) = \mu_s \int p(\hat{\mathbf{s}}, \hat{\mathbf{s}}')A(\hat{\mathbf{s}}')d^2s'$$

We expand the amplitdude A into locally-rotated spherical functions:

$$A(\hat{\mathbf{s}}) = \sum_{l,m} C_{lm} Y_{lm}(\hat{\mathbf{s}}; \hat{\mathbf{k}})$$

Here $Y_{lm}(\hat{\mathbf{s}}; \hat{\mathbf{k}})$ is a spherical function in a reference frame whose z-axis coincides with the $\hat{\mathbf{k}}$ direction:

$$Y_{lm}(\hat{\mathbf{s}}; \hat{\mathbf{k}}) = \sum_{m'} D^l_{mm'}(\varphi, \theta, 0) Y_{lm'}(\hat{\mathbf{s}})$$

Evanescent modes for the RTE II

The coefficients C_{lm} are determined by solving the generalized eigenproblem

$$\sum_{l',m'} R^{lm}_{l'm'} C_{l'm'} = \lambda \sigma_l C_{lm} \ .$$

Here $\sigma_l = \mu_a + \mu_s(1 - p_l)$ and

$$R^{lm}_{l'm'} = \delta_{mm'} \left(b_{lm} \delta_{l',l-1} + b_{l+1,m} \delta_{l',l-1} \right) \ ,$$

with $b_{lm} = \sqrt{(l^2 - m^2)/(4l^2 - 1)}$.

The generalized eigenproblem for R can be transformed to an eigenproblem for a symmetric block tridiagonal matrix $W = S^{-1} R^{-1} S^{-1}$ where $S^{l'm'}_{lm} = \delta_{ll'} \delta_{mm'} \sqrt{\sigma_l}$.

Evanescent modes for the RTE III

- There is a discrete and continuous spectrum of eigenvalues and a corresponding orthonormal basis of eigenvectors of W.
- For isotropic scattering, the three term recurrence relation for the tridiagonal matrix W is solved by the Legendre functions.
- The Henyey-Greenstein phase function with

$$p(\hat{\mathbf{s}}, \hat{\mathbf{s}}') = \frac{1}{4\pi} \sum_l (2l+1) g^l P_l(\hat{\mathbf{s}} \cdot \hat{\mathbf{s}}')$$

leads to a new family of orthogonal polynomials.

Green's functions for the RTE

In three-dimensions with planar boundaries, the Green's function can be written in the form

$$G(\mathbf{r},\hat{\mathbf{s}};\mathbf{r}',\hat{\mathbf{s}}') = \int \frac{d^2q}{(2\pi)^2} \sum_{lm,l'm'} g_{lm}^{l'm'}(z,z';\mathbf{q}) e^{i\mathbf{q}\cdot(\boldsymbol{\rho}-\boldsymbol{\rho}')} Y_{lm}(\hat{\mathbf{s}}) Y^*_{l'm'}(\hat{\mathbf{s}}') \ ,$$

where

$$g_{lm}^{l'm'}(z,z';\mathbf{q}) = \sum_{\mu} \sum_{M,M'} \Psi^{\mu}_{lm} \Psi^{\mu}_{l'm'} D^{l}_{mM}(\varphi,\theta,0) D^{l'}_{m'M'}(\varphi,\theta,0) \exp\left[-Q_\mu(q)|z-z'|\right]$$

and $Q_\mu(\mathbf{q}) = \sqrt{q^2 + 1/\lambda_\mu^2}$.

Ψ^μ and λ_μ are solutions to an eigenproblem for a tridiagonal matrix. D^l_{mM} are Wigner functions for $SO(3)$.

The dependence on $(\mathbf{r},\hat{\mathbf{s}})$ is analytical and the expansion can be obtained for any phase function.

Angular measurements

The intensity measured in an experiment is given by the expression

$$I = \int A(\hat{\mathbf{s}}) I(\mathbf{r}, \hat{\mathbf{s}}) \hat{\mathbf{s}} \cdot \hat{\mathbf{n}} d^2 s \ ,$$

where A accounts for the angular dependence of the optical system.

Two special cases are of interest:

- $A(\hat{\mathbf{s}}) = \delta(\hat{\mathbf{s}} - \hat{\mathbf{n}})$. This corresponds to a flat surface where the camera is at infinity; the aperture selects only normally oriented rays.
- $A(\hat{\mathbf{s}}) = 1$. This corresponds to complete angular data.

Inverse problem

The inverse transport problem of recovering the pair (μ_a, μ_s) with complete angular data is well-posed.

If incomplete or angularly averaged data is available, as is the case in experiments, the inverse problem is severely ill-posed. Low frequency components of (μ_a, μ_s) can be reconstructed with Holder stability.

Fourier-Laplace structure of the RTE

Recall the linearized integral equation for $\phi(\mathbf{r}_1, \hat{\mathbf{s}}_1; \mathbf{r}_2, \hat{\mathbf{s}}_2)$. Using the plane-wave decomposition of the Green's function and accounting for the angular dependence of the measurements, it can be seen that the Fourier transform of $\phi_A(\mathbf{r}_1, \mathbf{r}_2) = \int A(\hat{\mathbf{s}}_2)\phi(\mathbf{r}_1, -\hat{\mathbf{n}}; \mathbf{r}_2, \hat{\mathbf{s}}_2)d^2s_2$ is given by

$$\tilde{\phi}_A(\mathbf{q}_1, \mathbf{q}_2) = \sum_{\mu,\mu'} M_{\mu\mu'}(\mathbf{q}_1, \mathbf{q}_2) \int d^3r \exp\left[i(\mathbf{q}_1 - \mathbf{q}_2)\cdot\boldsymbol{\rho} - (Q_\mu(\mathbf{q}_1) + Q_{\mu'}(\mathbf{q}_2))z\right]\delta\mu_a(\mathbf{r}) \,,$$

where $\mathbf{r} = (\boldsymbol{\rho}, z)$ and we have assumed that the source is normally oriented.

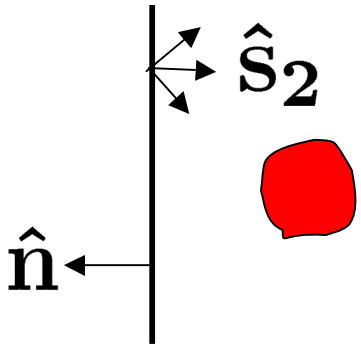

RTE vs diffusion (simulation)

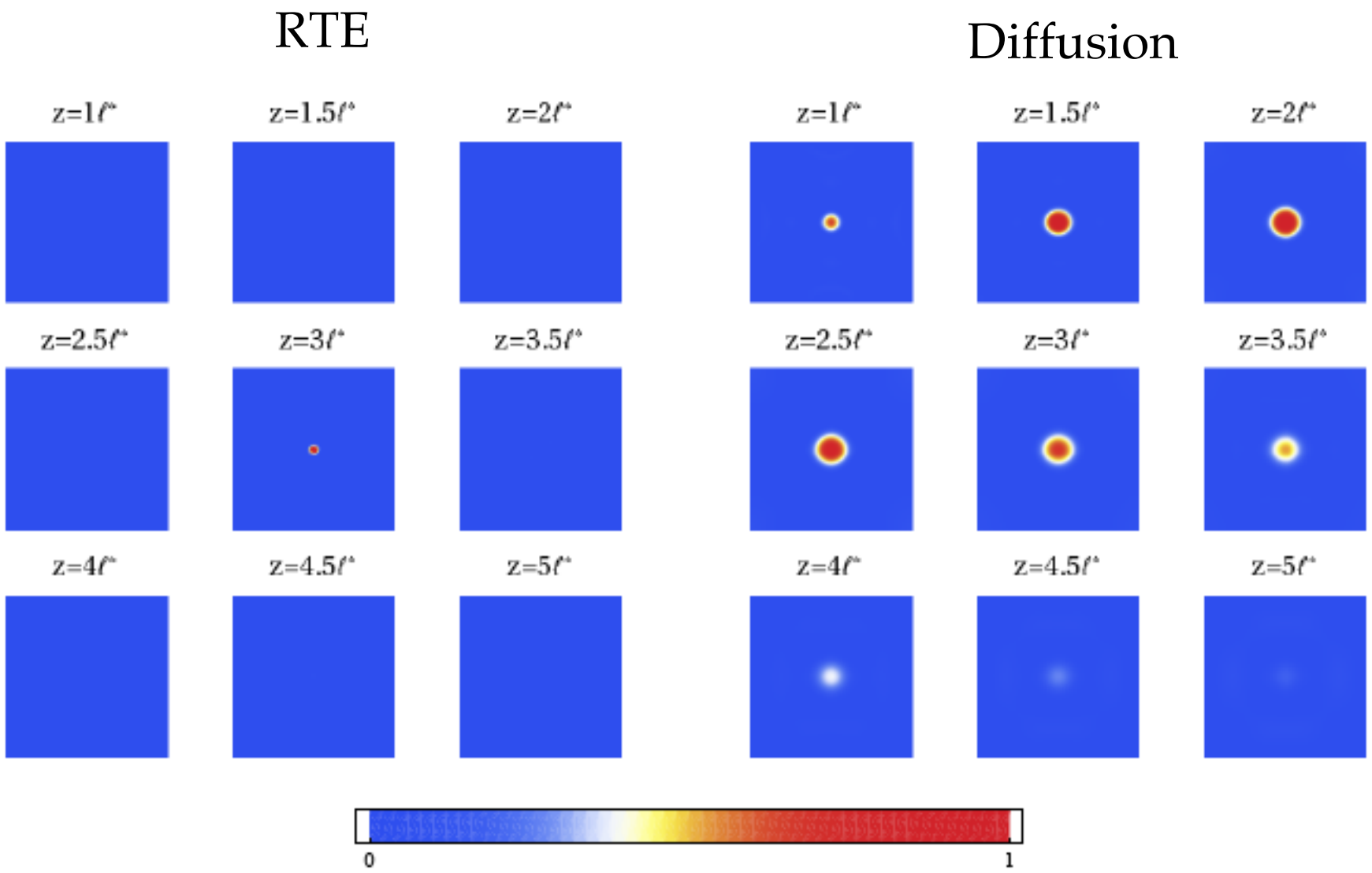

RTE (experiment)

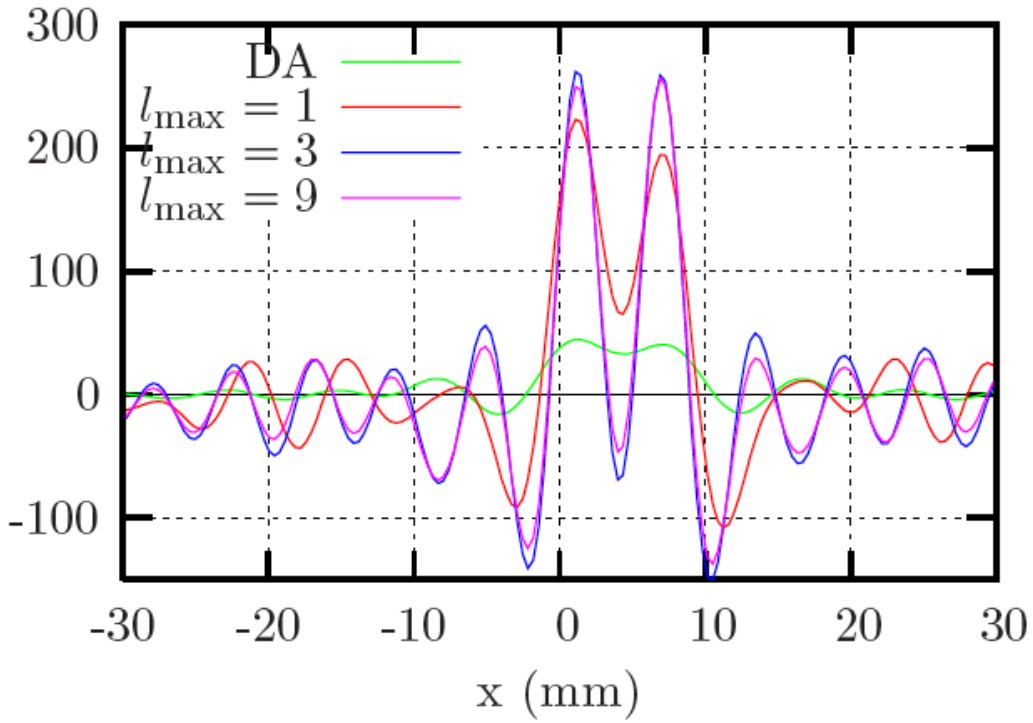

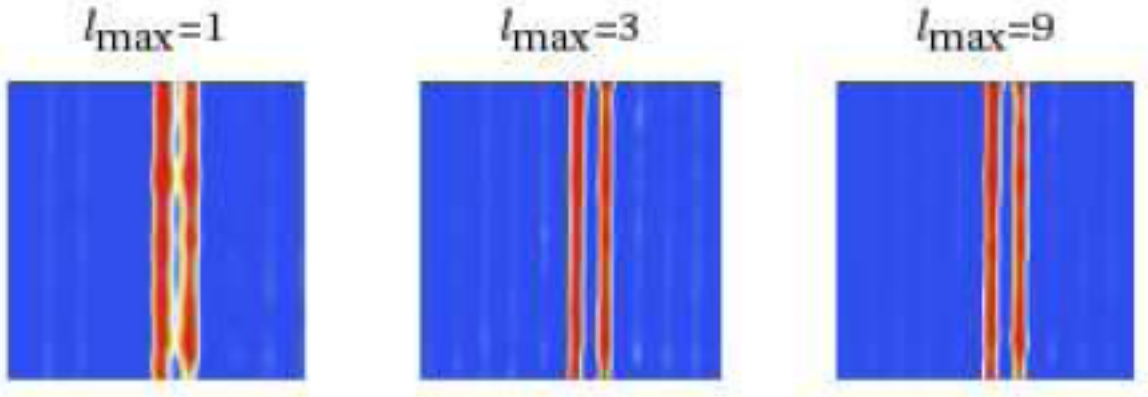

Structured illumination

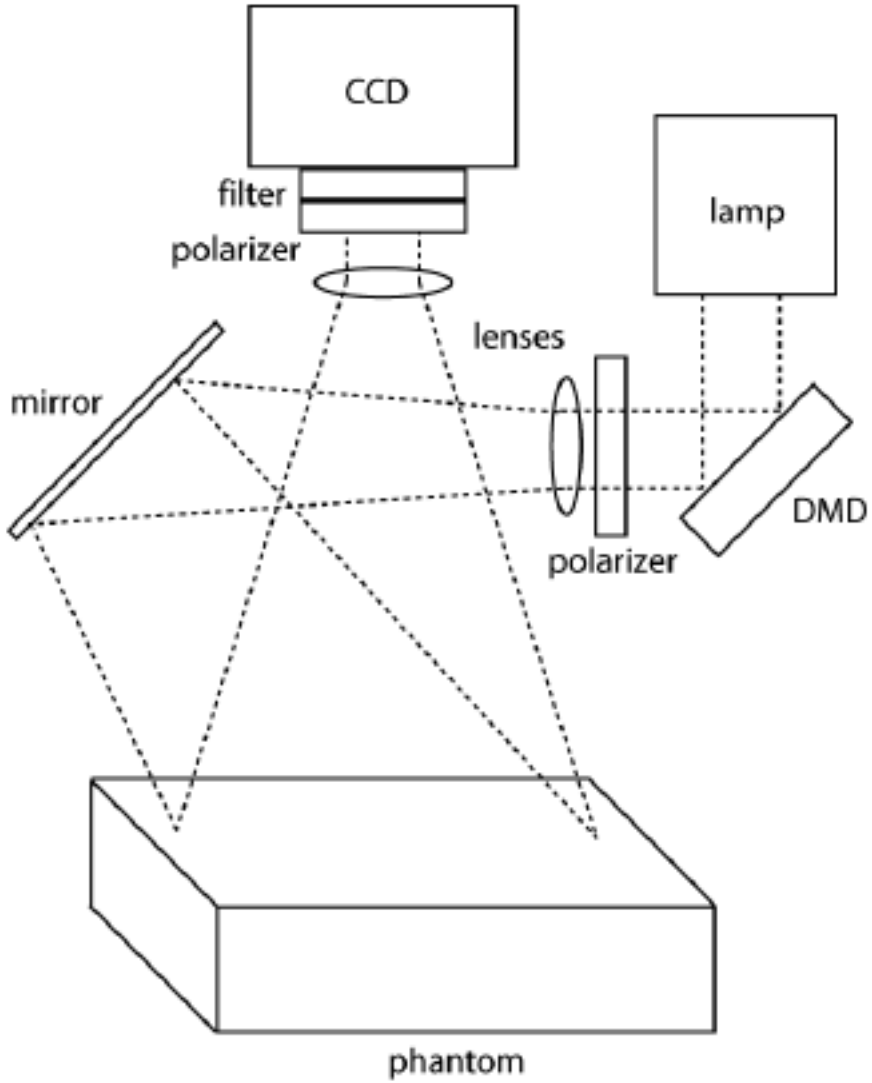

Structured illumination

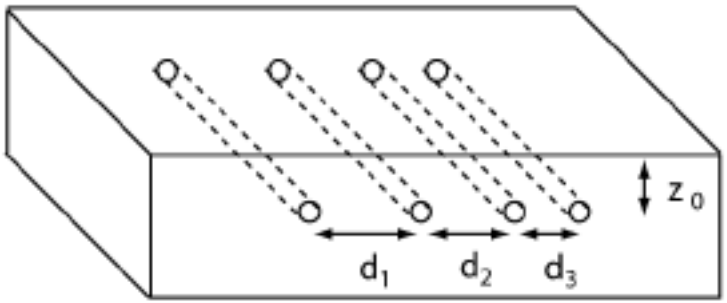

$z_0 = 3$ mm

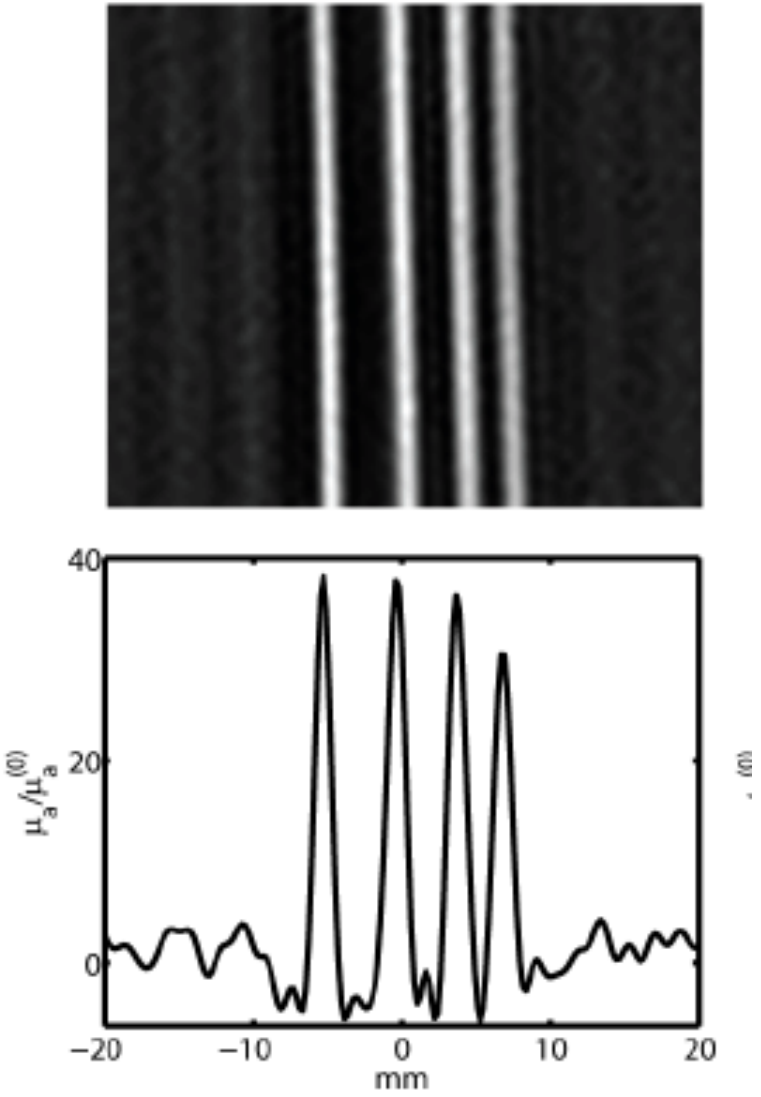

Lemon and lotus root